ISEE-1 DATA REDUCTION AND ANALYSIS PLASMA COMPOSITION EXPERIMENT

W Lennartsson
R. D. Sharp
Lockheed Missiles & Space Company, Inc.
Research and Development
3251 Hanover Street
Palo Alto, CA 94304

March 1985
Final Report
Contract NAS5-25773

Approved for Public Release:
Distribution Unlimited

Prepared for:
Goddard Space Flight Center
Greenbelt, MD 20771

TECHNICAL REPORT STANDARD TITLE PAGE

1. Report No.	2. Government Accession No.	3. Recipient's Catalog No.

4. Title and Subtitle
ISEE-1 DATA REDUCTION AND ANALYSIS
PLASMA COMPOSITION EXPERIMENT

5. Report Date

6. Performing Organization Code

7. Author(s)
W. Lennartsson and R. D. Sharp

8. Performing Organization Report No.
F018862

9. Performing Organization Name and Address
Lockheed Missiles & Space Company, Inc.
Research and Development
3251 Hanover Street
Palo Alto, CA 94304

10. Work Unit No.

11. Contract or Grant No.
NAS5-25773

13. Type of Report and Period Covered
Final Report

12. Sponsoring Agency Name and Address
Goddard Space Flight Center
Greenbelt, Maryland 20771
Technical Monitor: R. O. Wales, Code 602

14. Sponsoring Agency Code

15. Supplementary Notes

16. Abstract The ISEE-1 spacecraft offered the first opportunity to measure the energetic ion composition over a wide radial range in the near-equatorial magnetosphere, from close to the earth to a distance of almost 23 R_E. The Plasma Composition Experiment covers energies from 0 eV to 17 keV/e and has a mass-per-charge range from less than 1 to about 150 amu. Measurements have been made from the inner ring current region to the plasma sheet, magnetotail lobes, and the magnetopause boundary layers and beyond. Possibly the most significant results from the experiment are those related to energetic O^+ ions of terrestrial origin. These ions are found in every region of the magnetosphere reached by the spacecraft and can have energy and pitch-angle distributions that are similar to those traditionally associated with protons of solar wind origin. The O^+ ions are commonly the most numerous ions in the 0.1 - 17 keV/e energy range at $L < 5$ and are often a substantial part of the ion population at larger distances as well, especially during geomagnetically disturbed conditions. This report is an overview of results obtained for the O^+ and other ions with energies in the 0.1 - 17 keV/e range in the magnetosphere, and it also has a bibliography of scientific papers based on these results.

17. Key Words (Selected by Author(s))	18. Distribution Statement
Ion composition, Ring Current Ions, Plasma Sheet Ions, Magnetosphere Ions, Ion Streams, Energetic Ions, Ion Injection	

19. Security Classif. (of this report)	20. Security Classif. (of this page)	21. No. of Pages	22. Price*
Unclassified	Unclassified	78	

*For sale by the Clearinghouse for Federal Scientific and Technical Information, Springfield, Virginia 22151.

PREFACE

This report is an overview of the scientific results that have been obtained by the Plasma Composition Experiment on the ISEE-1 spacecraft. The experiment is designed to measure the differential flux of positive ions in the energy range from 0 eV to approximately 17 keV per unit charge. In contrast to the more conventional electrostatic particle analyzers flown on many spacecraft this experiment has the capability of selecting the ions to be measured by selecting the mass per unit charge. Only a few experiments of this type had been flown prior to the launch of ISEE-1 on October 22, 1977, and none had been flown across the same large region of the near-equatorial magnetosphere that is accessible to ISEE-1.

In the early years of space exploration, it was commonly presumed that the energetic plasma in the earth's magnetosphere, that is plasma with energies well above a few eV, was entirely of solar origin, being continuously supplied by means of the solar wind and gaining energy through complex interactions with the earth's magnetic field. This picture essentially reflected the popular theoretical concepts of that time and implied that the average energetic ion population in the magnetosphere should have a composition similar to what had been inferred in the solar wind, where all ions flow at nearly the same speed and different masses therefore can be recognized by their different characteristic energies. This average composition was expected to be about 95 -96% protons, 4 - 5% alpha particles, and only minor traces of heavier ions. However, the introduction of plasma composition experiments have fundamentally altered this picture by showing that the magnetosphere can have a large, and in many cases even dominant, component of energetic O^+ ions of terrestrial origin. These observations have made it necessary to reevaluate the existing theoretical concepts and to search for physical processes that may have been overlooked in the past.

In all regions of the magnetosphere reached by the ISEE-1 spacecraft, that is within about 23 R_E distance from the earth, the energetic ions have been observed to be a mixture of terrestrial and solar wind ions, and in some regions, notably in the inner magnetosphere and in the magnetotail lobes, the terrestrial ions may be dominant most of the time. The O^+ ions, in particular, have been observed to be accelerated and injected into the various parts of the magnetosphere in conjunction with increased geomagnetic activity,

suggesting a close association with the electric currents that flow between the outer magnetosphere and the polar regions of the earth's ionosphere at these times. Because the O^+ ions are almost completely of terrestrial origin, having started out with energies of only a few eV or less, their space and velocity distributions as observed in the outer magnetosphere may be our best source of information about the particle acceleration processes associated with these currents.

A particular strength of the ISEE mission has been the cooperative studies of data from many different kinds of experiments. These studies have also demonstrated the importance of ion composition data as a diagnostic tool for interpreting other kinds of data. In view of the vast amount of data that has been acquired by the various instruments on the ISEE-1, -2, and -3 spacecraft, and the unique character of much of these data, it is strongly recommended that continued support be provided for the ISEE data analysis for several more years.

TABLE OF CONTENTS

Section	Page
LIST OF ILLUSTRATIONS	1
LIST OF TABLES	5
INTRODUCTION	6
BRIEF DESCRIPTION OF THE EXPERIMENT	7
SCIENTIFIC RESULTS FROM THE MAGNETOTAIL	8
SCIENTIFIC RESULTS FROM THE INNER MAGNETOSPHERE	34
SCIENTIFIC RESULTS FROM THE MAGNETOSPEHRIC BOUNDARY REGIONS	54
NEW TECHNOLOGY	56
CONCLUSIONS	57
RECOMMENDATIONS	59
REFERENCES	60
ACKNOWLEDGMENTS	67
BIBLIOGRAPHY	68

LIST OF ILLUSTRATIONS

Figure		Page
1.	Comparative H^+ and He^{++} spectrums in the plasma sheet at 15 R_E geocentric radial distance. The data have been averaged over 360° and plotted versus energy per charge.	11
2.	Comparative H^+ and He^{++} spectrums in the plasma sheet at 21 R_E geocentric radial distance. The data have been averaged over 360° and plotted versus energy per nucleon.	12
3.	Distributions of ratios of He^{++}/H^+ densities in the plasma sheet during quiet and active times. The data cover the energy per charge range from 0.1 to 16 keV/e. The mean values of the distributions and their standard deviations are shown in parenthesis.	14
4.	Distributions of ratios of O^+/H^+ densities in the plasma sheet during quiet and active times. The data cover the energy range from 0.1 to 16 keV. The mean values of the distributions and their standard deviations are shown in parenthesis. The inset shows an expanded plot of the results for density ratios < 0.1 during quiet times.	15
5.	Plasma sheet ion density ratios in the energy range 0.1 - 16 keV/e. The angled brackets <> denote averages over different samples, and the error bars represent the statistical uncertainties of the averages. The AE is sorted into discrete bins bordered by the tic marks on the horizontal axes.	20
6.	Average energies. The dashed line in the second panel indicates an energy 4 times larger than the H^+ energy.	21
7.	Estimates of true bulk energies ($\bar{E}_{H^+}$ multiplied by 4) using a Maxwell-Boltzmann function to approximate the measured distribution.	22

Figure		Page
8.	Number densities averaged over time intervals ranging from about 17 min to 60 min in length. Each interval corresponds to a horizontal section on the historgrams. The circular and triangular symbols indicate what fraction of the density of each population is due to narrowly collimated beams. The error bars show the propagated uncertainty in the counting statistics ($\pm$ 1σ). The vertical lines extending from top to bottom indicate the times of prominent changes in the auroral electrojet activity, as determined by groundbased magnetometers.	24
9.	O^+ streams in the plasma sheet observed on March 2, 1978.	26
10.	Distributions of ion streams with respect to the ion velocity at the peak flux intensity.	28
11.	Distributions of ion streams with respect to peak flux intensity.	29
12.	Distributions of ion streams with respect to the observed full widths at half maximum of their angular distributions.	30
13.	Angular distributions of 628 eV O^+ ions and 212 eV H^+ ions in a tail lobe stream on April 19, 1978 at 0500 UT. These are the energies corresponding to the peak response for the respective species.	33
14.	Distribution of fractional densities of O^+, He^+ and He^{++} in the inner magnetosphere (2-15 R_E geocentric distance) during magnetic storms.	36
15.	Phase space density distributions exhibiting a "hole" in the few keV range.	38
16.	Schematic illustration of a relationship between measured energy and spatial origin of ions.	39

Figure		Page
17.	Energy at deepest minimum in phase space density distribution as a function of geocentric distance, for O^+ ions on December 11, 1977 (solid line) and energy at which co-rotation cancels gradient B drift (dashed line).	40
18.	O^+/H^+ density ratios during storms as a function of geocentric distance. Upper limits are indicated by open symbols. Triangles represent data in the 0100 to 0600 LT sector and circles represent data in the 0600 to 0100 LT sector. The two histograms to the right show the total number of points in the indicated vertical bins for $R > 7\ R_E$. The solid histrogram corresponds to the 0100 to 0600 LT data and the dashed histogram to the 0600 to 0100 LT data.	42
19.	He^{++}/H^+ density ratios in the same format as Figure 14.	43
20.	Average O^+/H^+ density ratios as a function of L for quiet and disturbed conditions.	45
21.	Average He^+/H^+ density ratios as a function of L for quiet and disturbed conditions.	46
22.	Average He^{++}/H^+ density ratios as a function of L for quiet and disturbed conditions.	47
23.	H^+ energies and densities measured during two successive traversal of the dayside magnetosphere during a major magnetic storm, along with theoretical predictions for the second traversal based on charge exchange decay of the measured ions from the first traversal (see text).	49
24.	Same as Figure 23 but showing data for the O^+ (and some data for the He^+).	50

Figure | Page

25. Phase space densities in the magnetosheath averaged over a 60^{o} interval centered on the bulk flow direction and plotted against total energy in the center of mass frame. The data were acquired on 19 November, 1977 between 2330-2359 UT when ISEE was located between 13.7 and 13.2 R_E at~ 0955 local time. 55

LIST OF TABLES

Table		Page
1	Measured Ion Density Ratios, $0.1 \leq E/q \leq 16$ keV/e	18
2	Statistical Study of Ion Beams in the Magnetotail	31
3	Relative Contribution of Ionospheric Ions	53

1. INTRODUCTION

This is the final report by the Lockheed Missiles & Space Company, Inc., Research and Development, to the National Aeronautics & Space Administration, Goddard Space Flight Center, under a contract to analyze and interpret data from the Plasma Composition Experiment on the International Sun-Earth Explorer spacecraft A (ISEE-1). The purpose of this report is to review the most significant scientific discoveries that have been made in the course of the data analysis and interpretation, and to provide a bibliography of scientific papers based on the data. In addition to the bibliography, which is limited to papers dealing specifically with the ISEE-1 plasma composition data, the report also has a list of references which contains various papers from the scientific literature that are especially relevant to the subject matter. References to this list are made by number in order of initial appearance.

1.1 Brief Summary of Scientific Results

ISEE-1 has carried the first energetic ion mass spectrometer to the distant magnetotail and some remarkable results have emerged from the experiment in that region. Within the plasma sheet a correspondence between the He^{++} and H^{+} spectrums in a number of instances has provided new information on the mechanisms involved in the entry and thermalization of the solar wind. A statistical study has shown a high fractional O^{+} content with increasing substorm activity and a simultaneously decreasing fraction of He^{++}. From these results one can infer that the ionosphere provides a comparable amount of the p lasma sheet to the solar wind during active times. A separate and distinct population of low intensity streaming ions of recent ionospheric origin exists in both the distant plasma sheet and the lobes of the magnetotail. Because of the limitations of earlier instruments they have not previously been identified. They form the dominant plasma constituent in the tail lobes and we therefore come to the unexpected conclusion that the hot plasma in this distant region of the magnetosphere is predominantly of ionospheric origin. In the inner magnetosphere ISEE has provided radial scans of the equatorially trapped plasma composition and given us new insight into the composition and dynamics of the ring current. A commonly observed spectral feature allows us to infer the typical gross plasma circulation pattern during major magnetic storms and thereby make the first indirect determination of the composition

and relative source strengths for the principal ring current ion population which is above the energy range of any currently operating ion mass spectrometers. We conclude that the solar wind is relatively more important in this higher energy portion of the spectrum than it is at energies per charge below 17 keV/e but that the ionosphere is still a significant contributor to the ring current even at high energies. A statistical study has provided a comparison of the ion composition in the near equatorial magnetosphere during quiet and disturbed conditions and allowed a test of the theoretical models for the decay of the storm time ring current. We conclude that current models based on the charge exchange decay of a static trapped population are inadequate to explain the observations. The experimental results suggest the need to add a continuous injection mechanism to the models, even during periods of extended quiet conditions, and to include transport effects with time constants which are not long compared to charge exchange lifetimes as is currently assumed.

2. BRIEF DESCRIPTION OF THE EXPERIMENT

The energetic ion mass spectrometer on the International Sun Earth Explorer (ISEE-1) is one of a family of instruments utilizing the same basic ion optics that have been, or are being, constructed for a number of projects including GEOS-1, GEOS-2, ISEE, Dynamics Explorer and AMPTE (Active Magnetospheric Particle Tracer Experiment). The basic instrument has been described in Refs. 1-3. It covers the energy per charge range from 0 to $\approx$ 17 keV/e and the mass range from 1 to $\sim$ 150 amu. It has high sensitivity ($\sim$ 1 cm^2 sr eV) and a resolution of $M/\Delta M \approx 10$ at focus.

Adapting the instrument to the requirements of the ISEE mission was a particular challenge because of the diverse nature of the plasmas encountered by ISEE-1 in its highly elliptical orbit. They include the cold, dense plasmas of the plasmasphere, the highly energetic ring current ions, the strongly flowing (high mach number) magnetosheath and boundary layer plasmas, the very tenuous tail lobe plasmas, the quasi-isotropic (low mach number) plasma of the plasma sheet, and the solar wind. The experiment has provided significant results in each of these regimes, in several of them for the first time with an ion mass spectrometer.

ISEE-1 was launched on 22 October 1977 into a geocentric elliptical orbit with apogee at an altitude of 138,120 km, perigee at 281 km, and an inclination of 28.7°. It has an orbital period of 2.4 days. It spins at about 2 RPM with its spin axis nearly normal to the ecliptic. The experiment view direction is approximately in the satellite spin plane.

The experiment is controlled through an onboard random access memory which can be programmed from the ground. Specialized modes have been developed for each plasma regime to satisfy evolving scientific objectives. A typical magnetospheric mode consists of a sequence of measurements of a few selected ion species with each element of the sequence consisting of a 4 second (480° of rotation) measurement at one of 16 energy steps. Other modes include the acquisition of more detailed energy and mass spectrums with up to 64 steps being available in each parameter.

The energy-per-charge range is normally divided into a "cold plasma" range from 0 eV/e to 100 eV/e, which is analyzed by a retarding potential analyzer, and a "hot plasma" range from 100 eV/e to 17 keV/e. This report is limited to data obtained in the "hot plasma" range and also limited to data obtained in the magnetosphere and the adjacent boundary regions. The "cold plasma" data in the energy range below 100 eV/e (Refs. 4 and 5) and the data from the solar wind (Ref. 6) are reported elsewhere.

3. SCIENTIFIC RESULTS FROM THE MAGNETOTAIL

ISEE-1 carries the first energetic ion mass spectrometer to be used in the distant magnetotail and some remarkable results have emerged from the initial studies of the composition of the plasma in that region. The experiment samples three principal magnetotail plasma regimes: the plasma sheet, the tail lobes, and the magnetospheric boundary layer. The plasma sheet is characterized by a high temperature plasma with kT of the order of a few keV and density in the range of a few tenths per cm^{-3}. The bulk flow energies are generally small compared to the thermal energies. The composition is generally dominated by H^+ ions during quiet times, but as we shall see below, a strong O^+ component appears with increasing substorm activity. Within this quasi-isotropic population we find a separate population of ion streams with low thermal energies compared to their bulk flow energies. The streams apparently originate in the auroral acceleration region at altitudes of $\sim$ 1 RE and

consist primarily of O^+ and H^+ ions. They have been studied extensively with the ion mass spectrometer experiment on the low altitude S3-3 satellite (see Refs.7-9). The H^+ component of the streams is often difficult to resolve from the low energy tail of the H^+ component of the quasi-isotropic population but the O^+ component is generally readily distinguishable.

The streams also exist in the tail lobes with properties similar to those of the streams in the plasma sheet. The streams are generally the dominant constituent of the tail lobe plasma in this energy range. We therefore come to the unexpected finding that the hot plasma in this distant region of the magnetosphere is predominately of ionospheric origin, energized by processes different from those producing the polar wind (cf. Ref. 10).

The third magnetotail plasma regime, the magnetospheric boundary layer, has been extensively studied with electrostatic analyzer experiments on previous satellites (refs. 11-14). The different ionic constituents are typically flowing at the same bulk velocity and have thermal energies which are low compared to their bulk flow energies so that even a non-mass discriminating instrument can often be used to infer the presence of the O^+ and H^+ components. We find that these boundary layer streams generally consist of H^+ and He^{++} ions in typical solar wind ratios with an occasional small O^+ component arising from an ionospheric acceleration process which has been observed to be operating in the polar cusp (Ref. 15).

In the following paragraphs we shall illustrate some of the characteristics of the magnetotail plasmas with examples and statistical results from the ISEE ion composition experiment.

3.1 Plasma Sheet.

Peterson et al. (Ref. 16) presented a detailed analysis of plasma sheet parameters for six specific intervals of $\sim$ 1 to 2 hours in duration when ISEE was at radial distances between 15 and 21 RE during the spring of 1978. The intervals were selected to illustrate the range and variability of the energetic ion composition.

In all the intervals except one, H^+ was the dominant constituent in the energy per charge range $\leq$ 17 keV/e. O^+ varied from 2.0% to 71% of the number density. He^{++} varied from 0.3% to 4.4% and He^+ was always less than 0.5%. In several instances a remarkable correspondence was found between the detailed shapes of the He^{++} and H^+ energy spectrums at high energies. This is illus-

trated for two of the intervals in Figures 1 and 2. In Figure 1 the data from the two ion species have been plotted on the same energy per charge scale, while in Figure 2 the abscissas have been shifted relative to each other by a factor of 2 so that they are on the same energy per nucleon scale. Other examples were found where the best correspondence was achieved if the abscissas were shifted by some value intermediate between those in Figures 1 and 2.

H^+ and He^{++} spectrums which are identical on an energy per nucleon scale are suggestive of a situation in which the solar wind plasma is injected into the magnetosphere by mass and charge independent processes preserving the relationship between the energy distributions which exists in the solar wind. He^+ and He^{++} spectrums which match well on an energy per charge scale suggest that mechanisms involving an electrostatic acceleration were involved in the injection process. It was concluded from these results that no single mechanism of solar wind entry and subsequent thermalization and acceleration was dominant at all times in the plasma sheet.

Peterson et al., (Ref. 16) also estimated the fraction of the plasma sheet number density of terrestrial (ionospheric) origin. The problem in making such an estimate is equivalent to estimating the fraction of H^+ of terrestrial origin, since it is reasonable to assume that all observed He^{++} is of solar origin and all observed O^+ is of terrestrial origin. The basis for estimating the fraction of H^+ of terrestrial origin is illustrated in Figure 1. In most of the intervals studied the distribution function of the He^{++} ions could be reasonably well approximated by a Maxwellian. The H^+ distribution function however often had an excess of ions at low energies in a region of the spectrum where O^+ ions of ionospheric origin made a substantial contribution.

Since the upflowing ion beams from the auroral acceleration region are known to contain both O^+ and H^+ ions it was inferred from these relationships that the low energy portion of the H^+ spectrum in excess of that predicted by a Maxwellian distribution was probably of ionospheric origin. An attempt was made to estimate the fractional ion density originating in the ionosphere (f_I) by summing these low energy protons with the O^+ and He^+ constituents. The values of f_I obtained for five of the intervals were: 0.10, 0.10, 0.25, 0.40, and 0.65.

A more extensive, statistical study of the plasma sheet composition has been performed utilizing data from the period March through May 1978

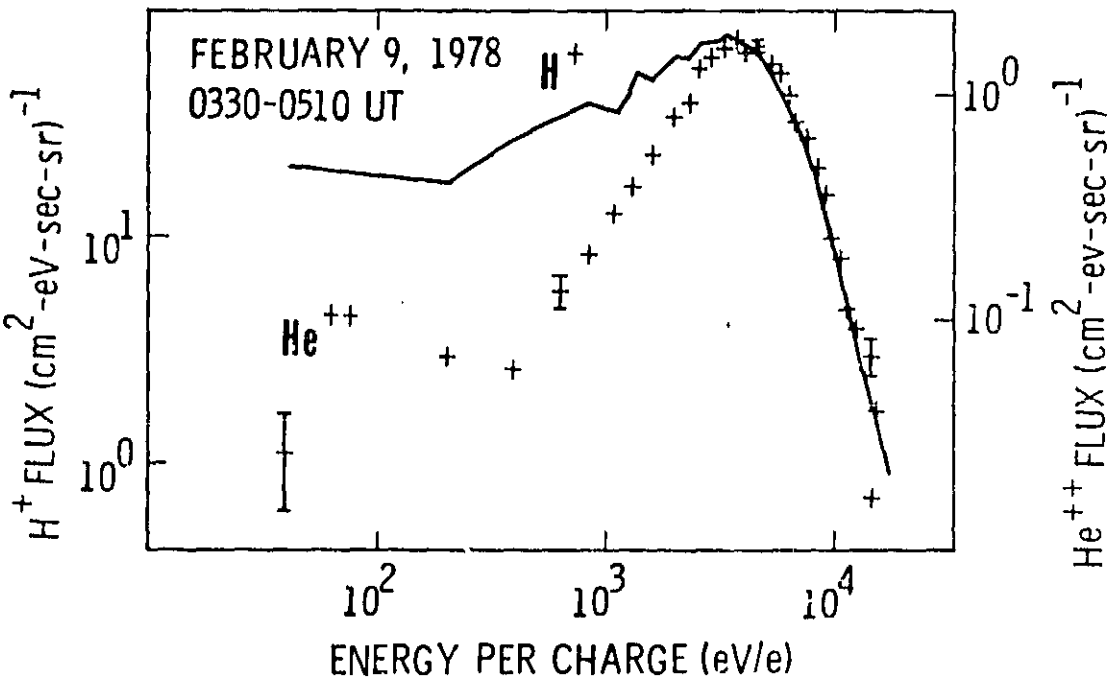

Figure 1. Comparative H^+ and He^{++} spectrums in the plasma sheet at 15 R_E geocentric radial distance. The data have been averaged over 360° and plotted versus energy per charge (Ref. 16).

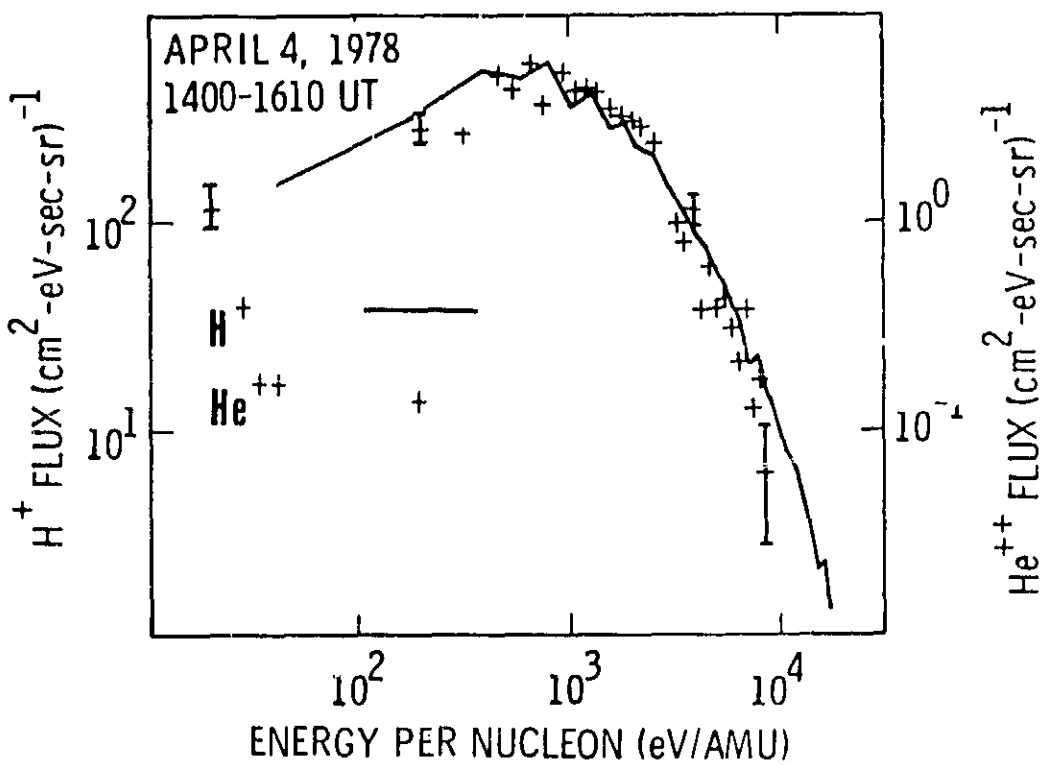

Figure 2. Comparative H^+ and He^{++} spectrums in the plasma sheet at 21 R_E geocentric radial distance. The data have been averaged over 360^o and plotted versus energy per nucleon (Ref. 16).

(Ref. 17). The relationship between the observed changes in composition and substorm activity has been studied by use of auroral electrojet indices (AE) provided by Kamei and Maeda (Ref. 18). Intervals of approximately 1 hour in duration when the spacecraft was continuously in the plasma sheet were identified from survey plots, and averages of the number densities and average energies of various ionic constituents were calculated. The data were integrated over pitch angle and over the energy per charge range from 0.1 to 16 keV/e. Periods when the satellite was in the lobes or magnetospheric boundary layer were excluded. The intervals are characterized as "active" if the AE index exceeds approximately 500 γ during the interval itself or the 1 hour period preceding it. Similarily they are characterized as "quiet" if the AE index does not exceed approximately 100 γ during the interval or the 1 hour period preceding it.

The data set consists of 40 quiet and 31 active intervals obtained on 16 different days when the spacecraft was between about 10 R_E and 23 R_E geocentric radial distance. The plasma in this energy range generally consisted almost entirely of H^+, O^+, He^{++} and He^+ and occasional small contributions of other species (e.g. O^{++}) were not included in the analysis. Histograms showing distributions with respect to the ratio of the number densities of He^{++}/H^+ and O^+/H^+ are shown in Figure 3 and 4. The He^{++}/H^+ ratio shows a small but significant decrease with increasing activity. The mean value of the ratio varies from .020 ± .002 (quiet) to 0.011 ± .002 (active). One should also note that the "active" distribution peaks in the lowest bin, whereas this bin contains no cases in the "quiet" distribution. As seen in Figure 4, the effect for O^+/H^+ is much more dramatic and in the opposite direction. The mean value of the ratio varies from 0.022 ± .003 (quiet) to 0.39 ± .06 (active). The He^+/H^+ ratio (not shown) also increases significantly with increasing activity. The mean value varies from 0.004 ± .001 (quiet) to 0.008 ± .001 (active).

As has been indicated previously the principal source regions for the plasma in the plasma sheet are thought to be the solar wind, which provides primarily H^+ and He^{++} ions, and the ionosphere, which provides H^+, O^+, and He^+ ions. The above results can be interpreted qualitatively as resulting from an increased contribution of the ionosphere relative to the solar wind as substorm activity increases. It would be of great interest if one could make this interpretation more quantitative and estimate the fraction of the number

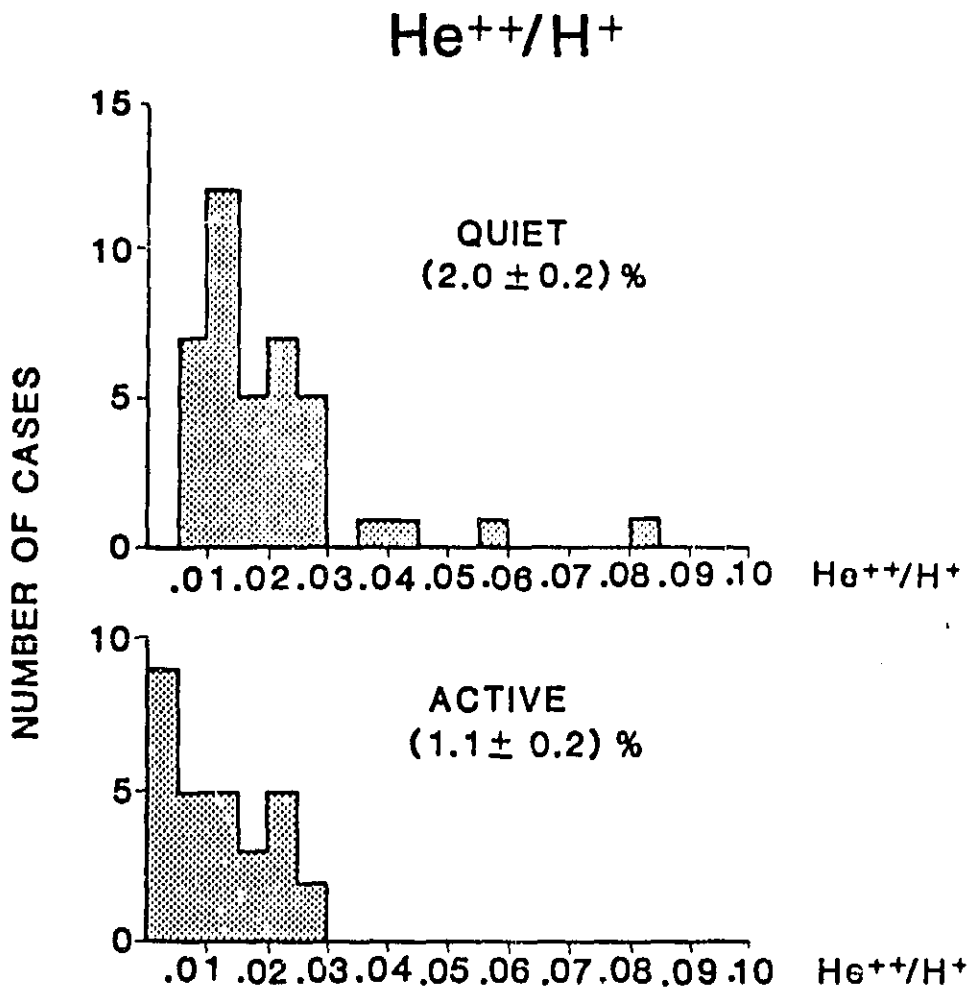

Figure 3. Distributions of ratios of He^{++}/H^{+} densities in the plasma sheet during quiet and active times. The data cover the energy per charge range from 0.1 to 16 keV/e. The mean values of the distributions and their standard deviations are shown in parenthesis (Ref. 17).

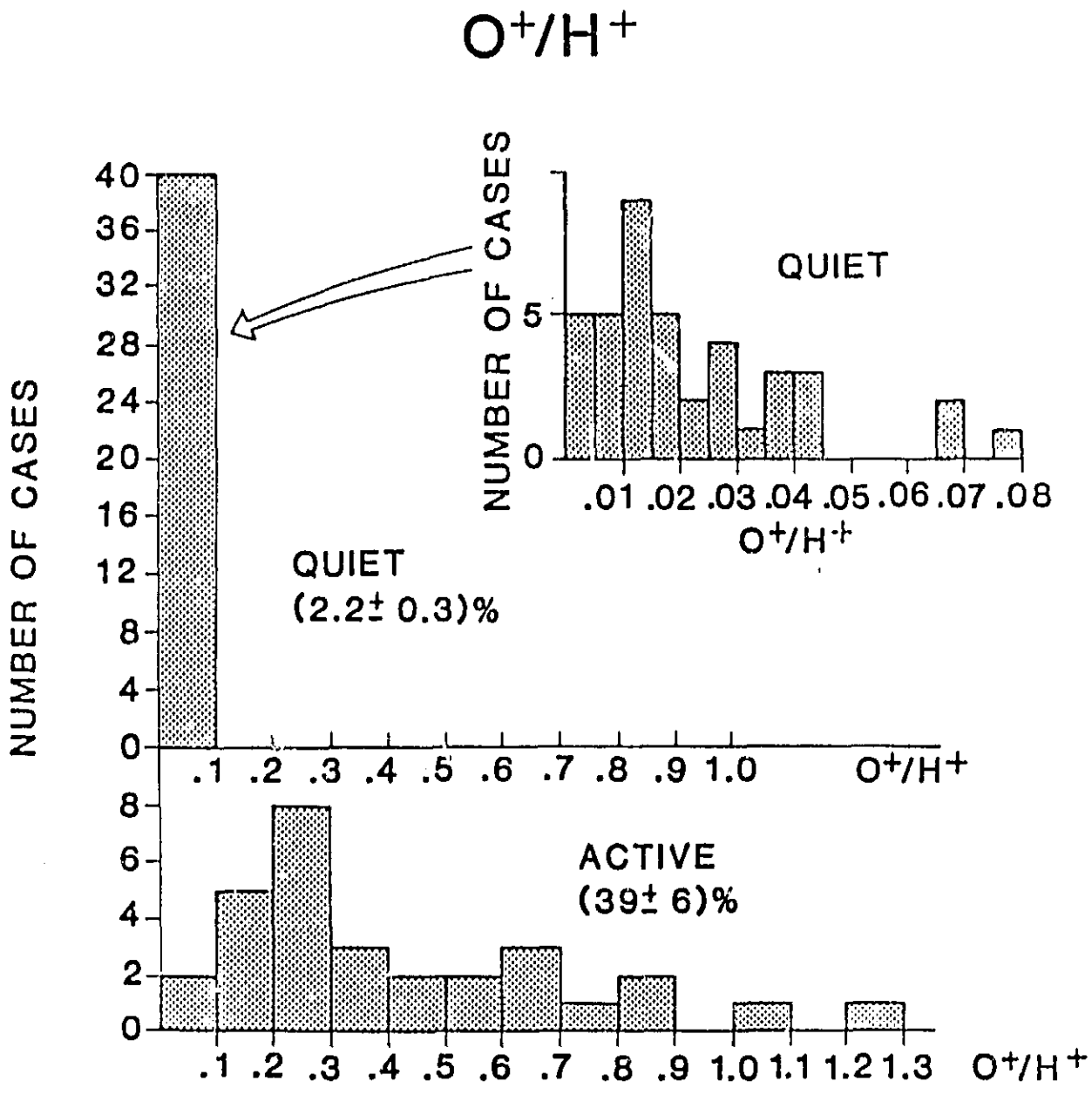

Figure 4. Distributions of ratios of O^+/H^+ densities in the plasma sheet during quiet and active times. The data cover the energy range from 0.1 to 16 keV. The mean values of the distributions and their standard deviations are shown in parenthesis. The inset shows an expanded plot of the results for density ratios < 0.1 during quiet times (Ref. 17).

density which can be attributed to each source. As outlined below, this is in fact possible if one is willing to make two principal assumptions.

We have 8 measured quantities, the number densities of the four principal species during active and quiet times: $H^+(A)$, $O^+(A)$, $He^{++}(A)$, $He^+(A)$, $H^+(Q)$, $O^+(Q)$, $He^{++}(Q)$, and $He^+(Q)$. As noted above, all the ions species except H^+ are essentially source specific so the problem reduces to determining the H^+ density originating in the ionosphere, ${H^+}_i(A)$, ${H_i}^+(Q)$; and in the solar wind, ${H_{sw}}^+(A)$, ${H_{sw}}^+(Q)$. We can solve directly for these four unknowns using the following 4 equations

$$ {H_i}^+(A) + {H_{sw}}^+(A) = H^+(A) \tag{1} $$

$$ {H_i}^+(Q) + {H_{sw}}^+(Q) = H^+(Q) \tag{2} $$

$$ \frac{O^+(Q)}{{H_i}^+(Q)} = \frac{O^+(A)}{{H_i}^+(A)} = X_1 \tag{3} $$

$$ \frac{He^{++}(Q)}{{H_{sw}}^+(Q)} = \frac{He^{++}(A)}{{H_{sw}}^+(A)} = X_2 \tag{4} $$

Equations 3 and 4 represent the principal assumption, i.e. that the ion composition of the two source terms does not vary systematically with substorm activity. Some evidence in support of Equation (3) has been presented by Shelley and coworkers (Ref. 19) and while not completely definitive it does strongly suggest that the O^+/H^+ ratio of the upflowing ion events does not vary appreciably with K_p. No published evidence exists either for or against the assumption in equation 4. It seems plausible however that short term fluctuations in AE are not dependent on the density of a minor constituent in the solar wind.

Simultaneously solving equations (1) through (4) we can compute X_1, X_2, and f_I, the fractional number density of ionospheric origin.

$$f_I = \frac{(O^+ + H_i^+ + He^+)}{(O^+ + H_i^+ + He^+) + (H_{sw}^+ + He^{++})} \qquad (5)$$

The input parameters and the results of the calculation are presented in Table 1. The indicated uncertainties represent counting statistics only. The results indicate that the plasma sheet was almost entirely of solar wind origin during quiet intervals but had an important, perhaps dominant, ionospheric contribution during the active periods. The plausibility of the solution can be examined by comparing the estimated values of X_1 and X_2 with previous measurements. Collin et al. (Ref. 9) studied upflowing energetic ions in the auroral zone with the S3-3 satellite over the period July 1976 to July 1977. Their results lead to an estimate of $X_1 = 0.25$, a factor of 3.5 lower than the value obtained here. Their results were for a somewhat different energy range ($0.5 \leq E/q \leq 16$ keV) and there is some evidence that the magnetospheric O^+/H^+ ratio has been increasing during the increasing phase of the solar cycle (Ref. 20) so this discrepancy does not appear to be unreasonable. Similarly the long term average value of X_2 in the solar wind is about 4% but the ratio varies widely (Ref. 21) and a value of 2.1% is not unreasonable.

TABLE 1. MEASURED ION DENSITY RATIOS, $0.1 \leq E/q \leq 16$ keV/e

	He^+/H^+	He^{++}/H^+	O^+/H^+
ACTIVE	.008 ± .001	.011 ± .002	.39 ± .06
QUIET	.004 ± .001	.020 ± .002	.022 ± .003

RESULTS OF CALCULATION

$X_1 = 0.87$
$X_2 = 0.021$
$f_I(A) = 0.60$
$f_I(Q) = 0.049$

As has been indicated, the results described apply only to the range $0.1 \leq E/q \leq 16$ keV/e and we must address the question of the uncertainity caused by those portions of the distributions outside this range. The plasma at lower energy was monitored by the instrument during these periods. The data come from a single wide-energy-band measurement ($.01 \leq E/q \leq .1$ keV/e) and have larger uncertainities than the higher energy data so they are not routinely included in the averages. The only significant contribution to the plasma density was for the quiet time O^+. An approximate correction for this contribution yields 0.031 for the O^+/H^+ ratio and raises $f_I(Q)$ to 0.067 with neglible change in the other results. The contribution at higher energies is more likely to be significant, particularly for the He^{++} which has the highest average energy per charge of the several species. To assess the magnitude of this uncertainity we extrapolated the number densities to higher energies by assuming a Maxwellian distribution which would produce the measured overall average energy for each species in the energy range of the measurements. The principal effect on the density ratios was for He^{++}/H^+ during active periods which increased to .017. Including these corrections gave $X_1 = 2.0$, $X_2 = .021$, $f_I(A) = .42$ and $f_I(Q) = .047$. The discrepancy with the Collin et al. (Ref. 9) results is seen to increase substantially but the estimates of relative source strengths are not greatly affected.

Quantitative estimates and limits on the ratio of hot plasma ions of terrestrial origin to those of solar wind origin near geosynchronous altitude have also been made by Balsiger et al (Ref. 22) and Johnson (Ref. 23) using

data from the ion composition experiment on the GEOS satellite in late 1978 and early 1979. Johnson (Ref. 23) also concludes that the ionospheric component of the plasma increases during magnetically disturbed periods. For Kp $\geq$ 3, using conservative assumptions for the ionospheric H^+ component, he infers that the ionospheric component is comparable to or exceeds the solar wind component, in agreement with the results for the distant plasma sheet reported here.

A much more extensive survey of the plasma sheet ion composition during varying geomagnetic conditions is presently underway, using all available data from 1978 and 1979. Some of the results obtained so far are presented in Figures 5-7, which are taken from Ref. 24. In this survey we have averaged the particle fluxes over time intervals that vary in length from 1 hour to as much as 3 hours, depending on the spacecraft position in the orbit (the longest intervals chosen near apogee). Despite the considerable length of these intervals the resulting number of independent plasma samples is close to 1000. This enables us to use a finer subdivision of the range of magnetic activity than was available in the previous studies. The AE indices plotted in these figures are based on the published hourly averages (Ref. 18 and following Data Books) and are chosen to be the maximum hourly AE during the averaging interval itself or the one hour preceding it.

The strong increase in the O^+/H^+ density ratio with increasing magnetic activity that was found in the previous studies is clearly demonstrated by the sample averages in Figure 5. In fact, the average O^+/H^+ ratio is roughly proportional to the AE index in this figure. Since the AE index is a measure of the substorm intensifications of the auroral electrojet currents, this figure also suggests that the acceleration and injection of O^+ into the plasma sheet are a direct consequence of the diversion of cross-tail currents through the ionosphere that is believed to be a central part of the substorm process (Ref. 25). The singly ionized helium, He^+, may also be associated with the same process but it shows a much weaker response to AE.

The alpha particles, He^{++}, on the other hand behave differently from the O^+ and the He^{++}/H^+ ratio appears to decline at very high activity levels, on the average. This is consistent with previous conclusions that the He^{++} is almost entirely of solar wind origin, whereas the H^+ also has a terrestrial component that is often enhanced during active conditions (Ref. 17). The different origins of the He^{++} and the O^+ ions may also be reflected in Figure

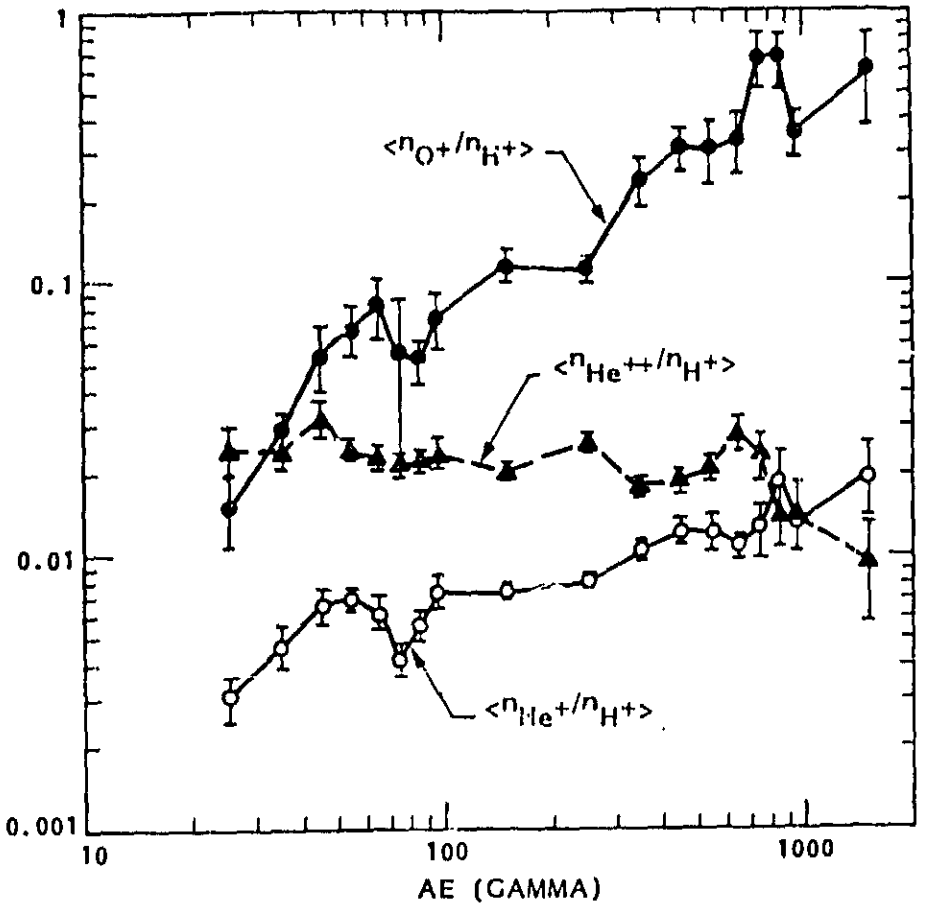

Figure 5. Plasma sheet ion density ratios in the energy range 0.1 - 16 keV/e. The angled brackets <> denote averages over different samples, and the error bars represent the statistical uncertainties of the averages. The AE is sorted into discrete bins bordered by the tic marks on the horizontal axes (Ref. 24).

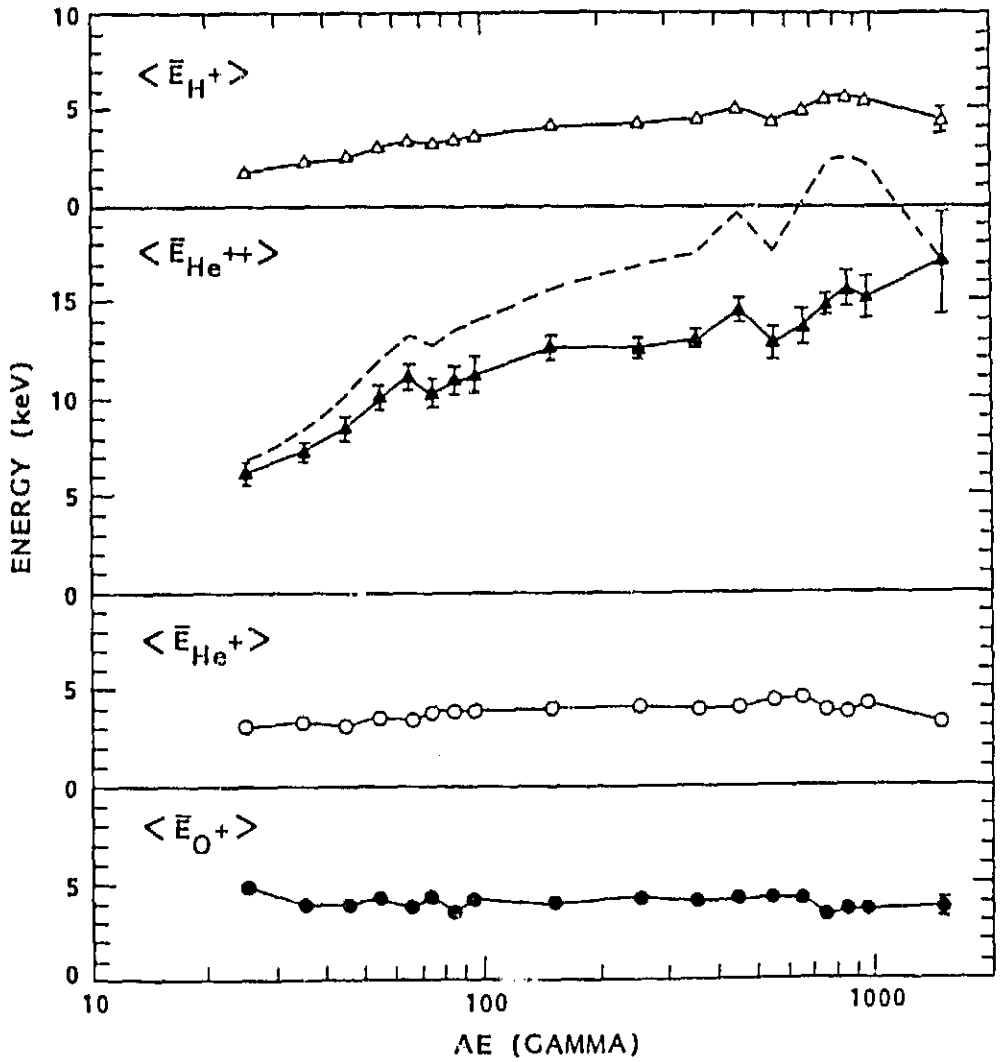

Figure 6. Average energies. The dashed line in the second panel indicates an energy 4 times larger than the H^+ energy (Ref. 24).

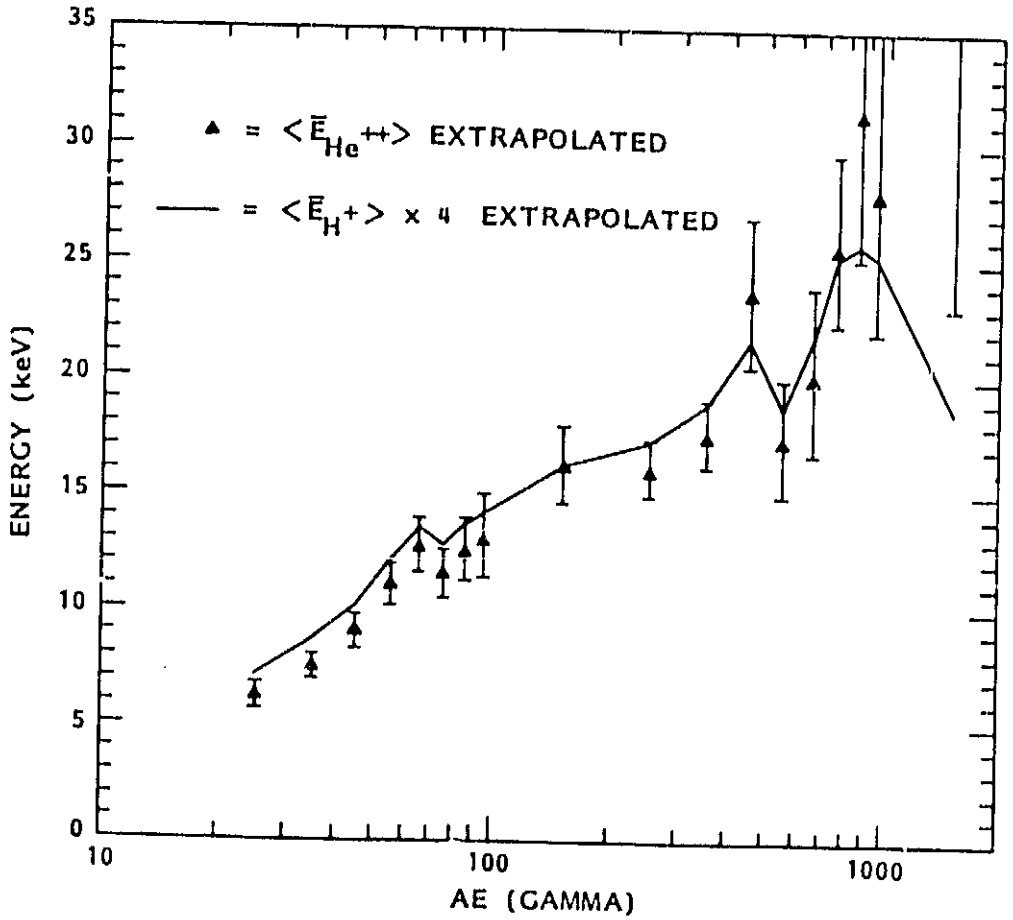

Figure 7. Estimates of true bulk energies ($\bar{E}_H^+$ multiplied by 4) using a Maxwell-Boltzmann function to approximate the measured distribution (Ref. 24).

6 (from Ref. 24), where the average energy of the He^{++} is seen to increase with increasing AE, whereas the O^{+} energy remains approximately constant (as does the He^{+} energy). The fact that the average energy of the H^{+} also increases with increasing AE apparently reflects a large or dominant component of solar wind origin. This is perhaps better illustrated in Figure 7 (Ref. 24), where a crude extrapolation has been made of the He^{++} and H^{+} energy distributions in order to compensate for the finite energy window of the instrument. It appears that the H^{+} and the He^{++} ions of solar wind origin may, on the average, have about equal energy per nucleon also in the plasma sheet, although the energies are significantly higher there than they are in the solar wind. This figure, which shows the averages of many samples, should be compared with Figures 1 and 2, which show two individual measurements. Apparently, the result in Figure 2 is more representative of average conditions than is the result in Figure 1.

The close relationship that seems to exist between magnetic substorm activity and the appearance of energetic O^{+} in the plasma sheet is very well illustrated by an event that was studied during the recent Coordinated Data Analysis Workshop (CDAW) 6. This event consisted of two intense substorms that occurred on March 22, 1979, after an extended period of magnetic quiet (over 48 hours of weak activity). The ion composition data obtained on this day by the ISEE-1 mass spectrometer are shown in Figure 8, which is taken from Ref. 26. The data from before 1000 UT were obtained well inside the plasma sheet, which at this time was presumably very thick in the GSM-z direction. The O^{+} ions (and the He^{+} ions) are a minor component of the plasma at this time, contributing less than 10% of the total ion density. After 1000 UT the plasma sheet underwent thinning and rapid motion in conjunction with the two substorms (expansion phase onsets at 1054 UT and 1436 UT, respectively), causing the ISEE-1 to approach the magnetotail lobes at times. Irrespective of the location of ISEE-1 relative to the center of the plasma sheet the O^{+} has become a large or dominant plasma component after about 1130 UT, soon after the expansion phase onset of the first substorm.

Possibly the most significant aspect of the change in ion composition between 1100 UT and 1200 UT in Figure 8 is the anti-correlation between the H^{+} and He^{++} ions on one hand and the O^{+} ions on the other. The H^{+} and He^{++} ions are thought to be predominantly of solar wind origin here and the O^{+} ions entirely of terrestrial origin (Ref. 26), implying a fundamental change in the

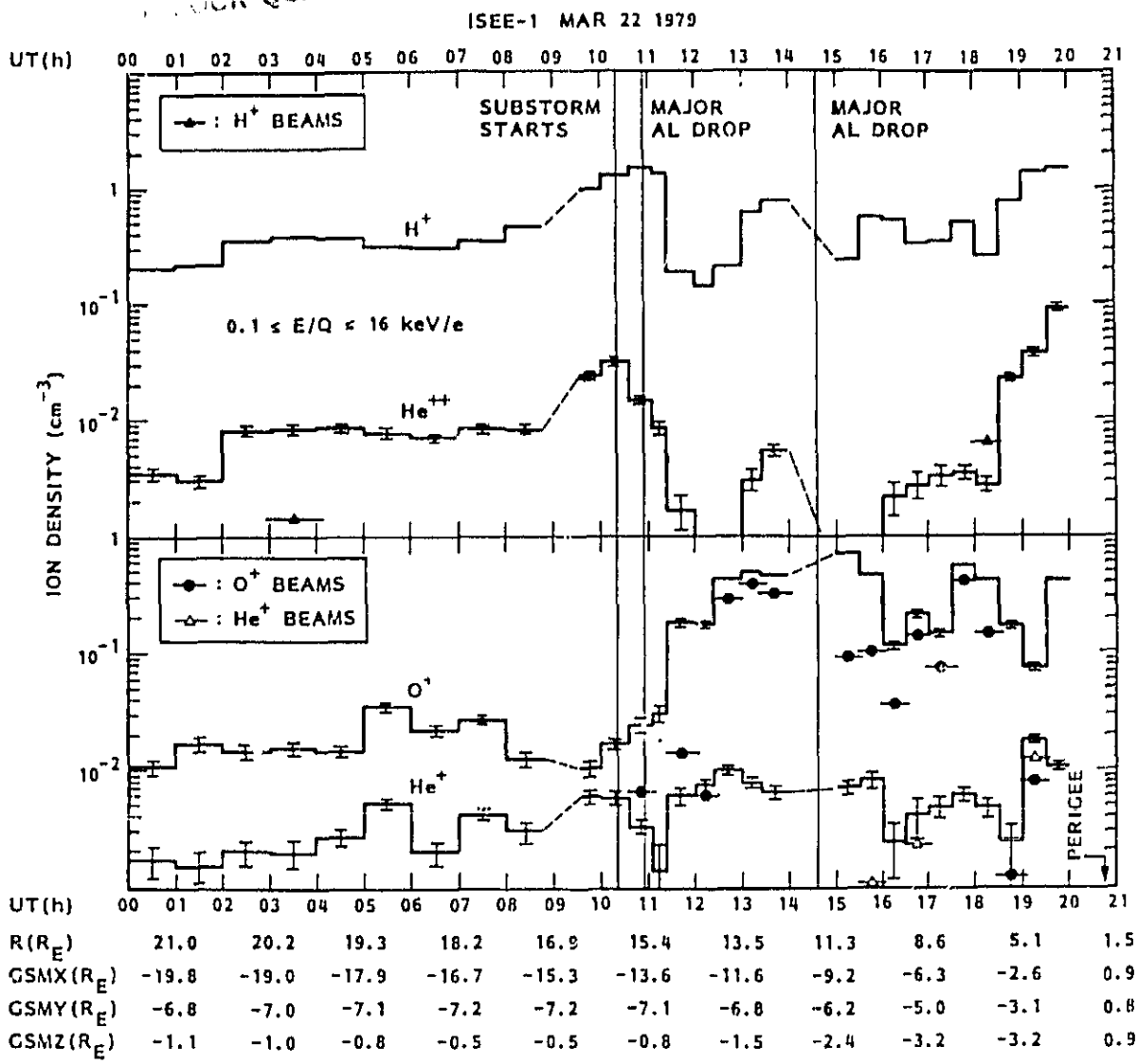

Figure 8. Number densities averaged over time intervals ranging from about 17 min to 60 min in length. Each interval corresponds to a horizontal section on the historgrams. The circular and triangular symbols indicate what fraction of the density of each population is due to narrowly collimated beams. The error bars show the propagated uncertainty in the counting statistics ($\pm 1\sigma$). The vertical lines extending from top to bottom indicate the times of prominent changes in the auroral electrojet activity, as determined by groundbased magnetometers (Ref. 26).

ion flow patterns associated with the substorm onset. This again suggests a physical relationship between the injection (and acceleration) of O^+ ions into the plasma sheet and the diversion of cross-tail currents through the ionosphere during substorms. A significant portion of the O^+ ions injected during these two substorms reached the ISEE-1 in the form of very intense and narrowly collimated beams or streams flowing tailward along the magnetic field lines, with energies ranging from a few hundred eV to several keV. Such streams have been observed previously by the ISEE-1 mass spectrometer, as discussed above, but they are not usually quite as intense. A further discussion of ion streams are given in the next section.

3.2 Ion Streams

As indicated above, a population of streaming ions of ionospheric origin, usually with low densities and temperatures, are observed throughout the magnetotail, both in the plasma sheet and the lobes. These streams usually consist either of O^+ or H^+ ions. They differ in their properties from both the primary plasma sheet plasmas and the boundary layer plasmas. The former are characterized by a quasi-isotropic pitch angle distribution and average energies of a few keV. The latter are generally more intense than the streams from the ionosphere and have an He^{++} component moving at the same bulk velocity as the dominant proton component. The boundary layers are usually confined to the vicinity of the magnetopause in the region of the magnetotail accessible to ISEE.

Figure 9 shows a data segment containing two O^+ streams in the plasma sheet observed at a geocentric radial distance of 22 R_E (Ref. 27). The 0.63 keV ions are flowing approximately tailward and the 1.6 keV ions are flowing approximately earthward. The spectrometer response is shown during three satellite spins when it was set on energy steps 1, 3, and 7 as indicated. The upper curve gives the pitch angle of the measured ions. The number density and temperature of the streams are estimated to be: $n = 4 \times 10^{-3}$ cm^{-3}, kT = 25 eV for the 0.63 keV stream and $n = 3 \times 10^{-3}$ cm^{-3}, kT = 96 eV for the 1.6 keV stream. These are well below the sensitivity threshold of previous experiments that have operated in this region of the magnetosphere. The quasi-isotropic plasma sheet population at this time consisted primarily of H^+ ions and had a number density of approximately 0.1 cm^{-3} and a temperature of approximately 5 keV. As indicated previously this population tended to

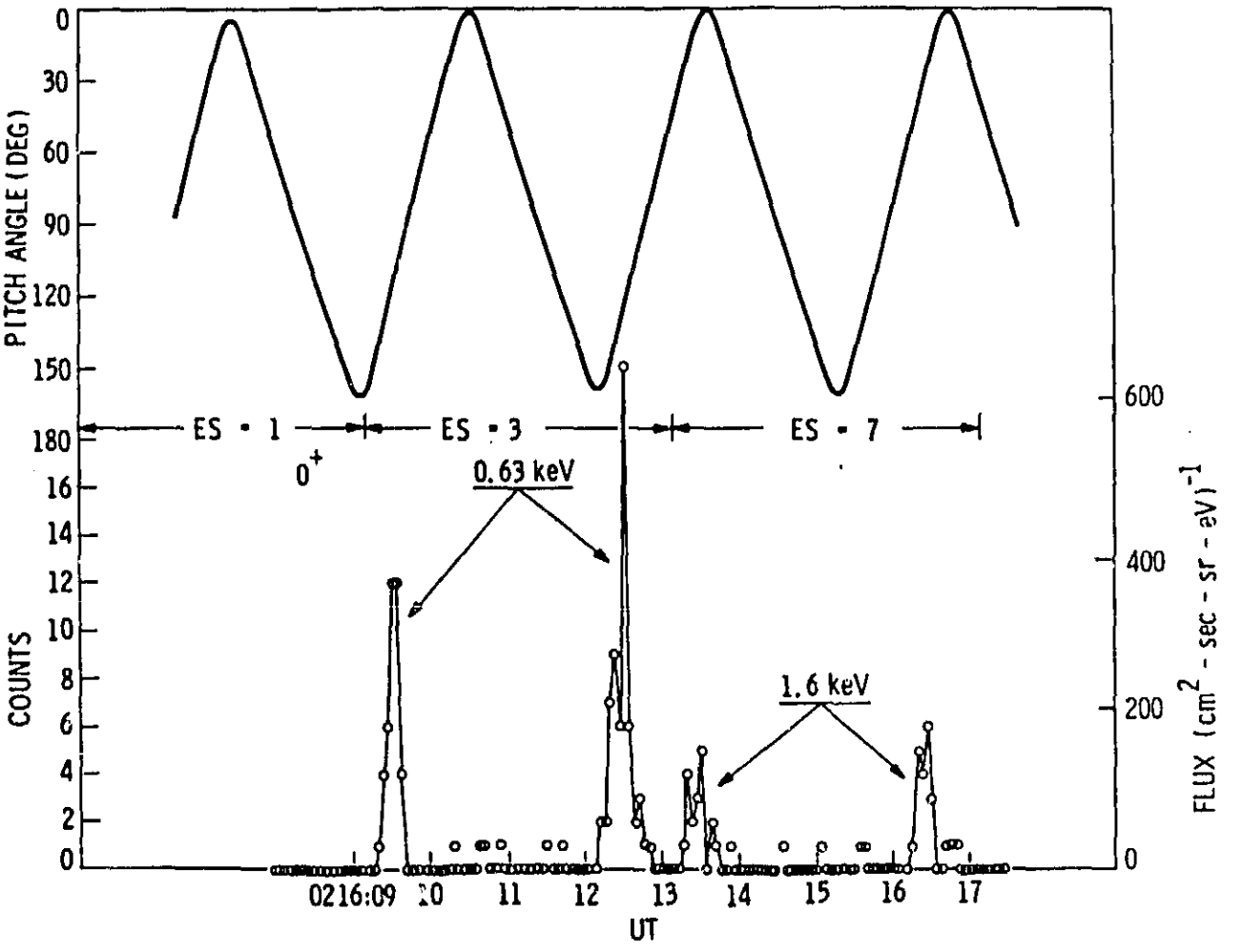

Figure 9. O^+ streams in the plasma sheet observed on March 2, 1978 (ref. 27).

obscure the weaker H^+ streams in the plasma sheet and for this reason the initial statistical studies dealt only with the O^+ streams in this region (Ref. 27).

These studies were based on approximately 134 hours of data during the period February-May 1978 when ISEE was in the expected location of the central plasma sheet and lobes. (Geocentric radial distance $\geq$ 11 R_E, $|GSMY| \leq 12\ R_E$, $|dZ| \leq 12\ R_E$). The principal results are illustrated in Table 2 and Figures 10, 11, and 12. Table 2 gives the frequency of occurrence based on the number of times the experiment sampled the given ionic constituent in the energy range (110 eV $\leq$ E/Q $\leq$ 17 keV). A division was made with respect to magnetic activity based on the Kp index and is indicated in the table. One sees that the overall frequency of occcurrence varied between $\sim$ 10% and 30%. O^+ was the most common constituent in the lobes. Increasing magnetic activity was related to a substantial increase in the plasma sheet streams and had a smaller effect in the lobes. For the H^+ streams in fact there was no discernible effect.

Figure 10 shows the distributions of the observed ion streams with respect to the energy step (top scale) at which there was maximum flux. The equivalent ion velocity is shown in the lower scales. One sees that the O^+ streams in the plasma sheet extend to significantly higher energies than in the lobes. The O^+ and H^+ distributions in the lobes are quite similar. The streams occur in the same general range of energies and not in overlapping ranges of velocity. This is one of the characteristics of the tail lobe streams that distinguishes them from the boundary layer streams.

Figures 11 and 12 show the distributions of peak flux intensities and angular widths of the observed streams. One sees a general similarity of the properties of the O^+ and H^+ in the lobes and of the O^+ streams in the lobes and plasma sheet. Although the statistics are poor there is some evidence in Figure 12 for a group of wide proton events in the lobes that are not evident in the O^+. The 112.5 to 120° bin represents a lower limit in that it includes some even wider examples, some of which had conical pitch angle distribution. As will be discussed below this may be the initial manifestation of a beam plasma instability which eventually thermalizes the tailward flowing lobe streams and injects them into the quasisotropic plasma sheet population.

The O^+ distribution in the lobes in Figure 11 shows a significant peak indicating that these streams have a somewhat higher average intensity than

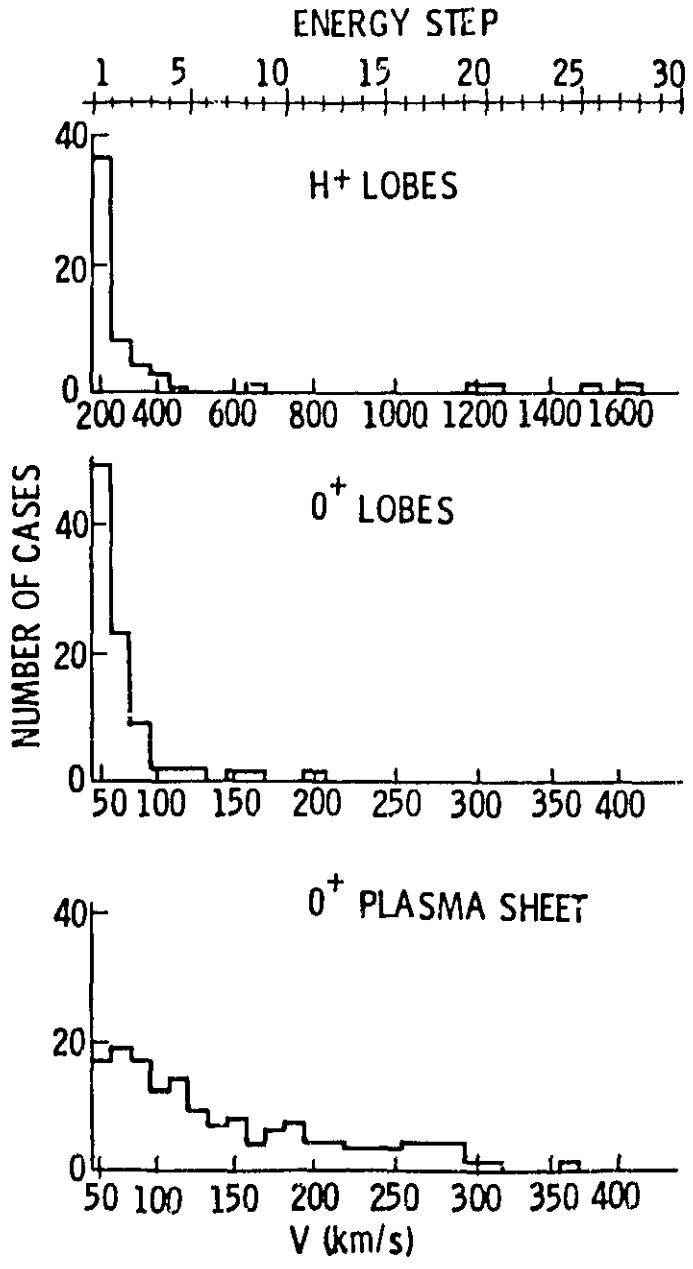

Figure 10. Distributions of ion streams with respect to the ion velocity at the peak flux intensity (Ref. 27).

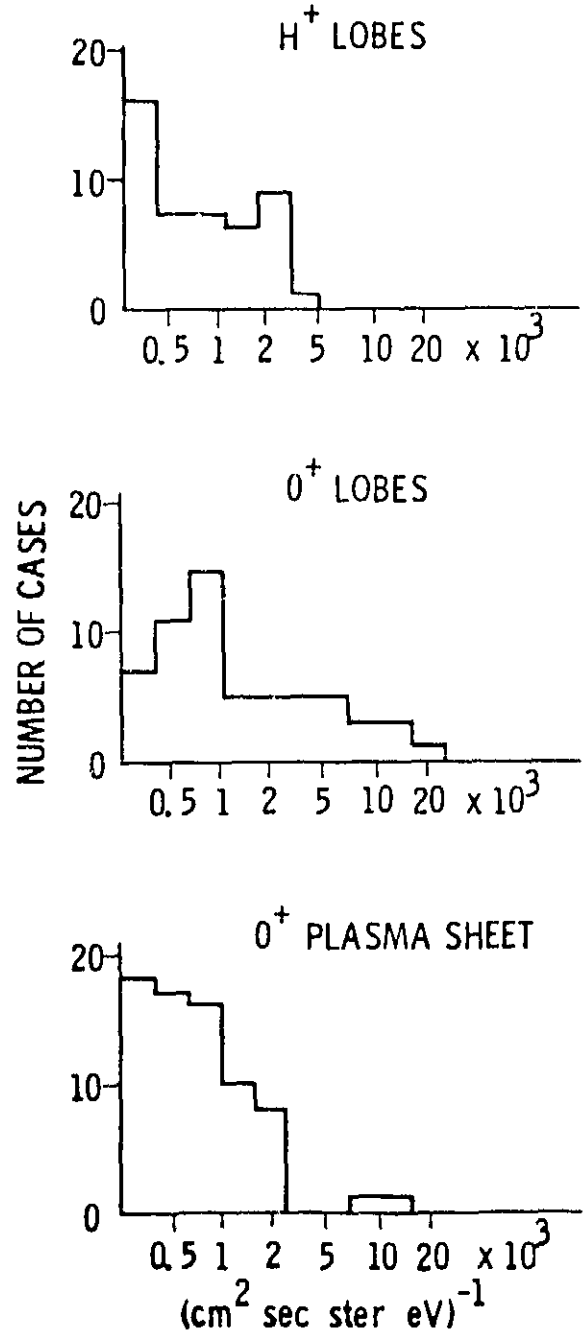

Figure 11. Distributions of ion streams with respect to peak flux intensity (Ref. 27).

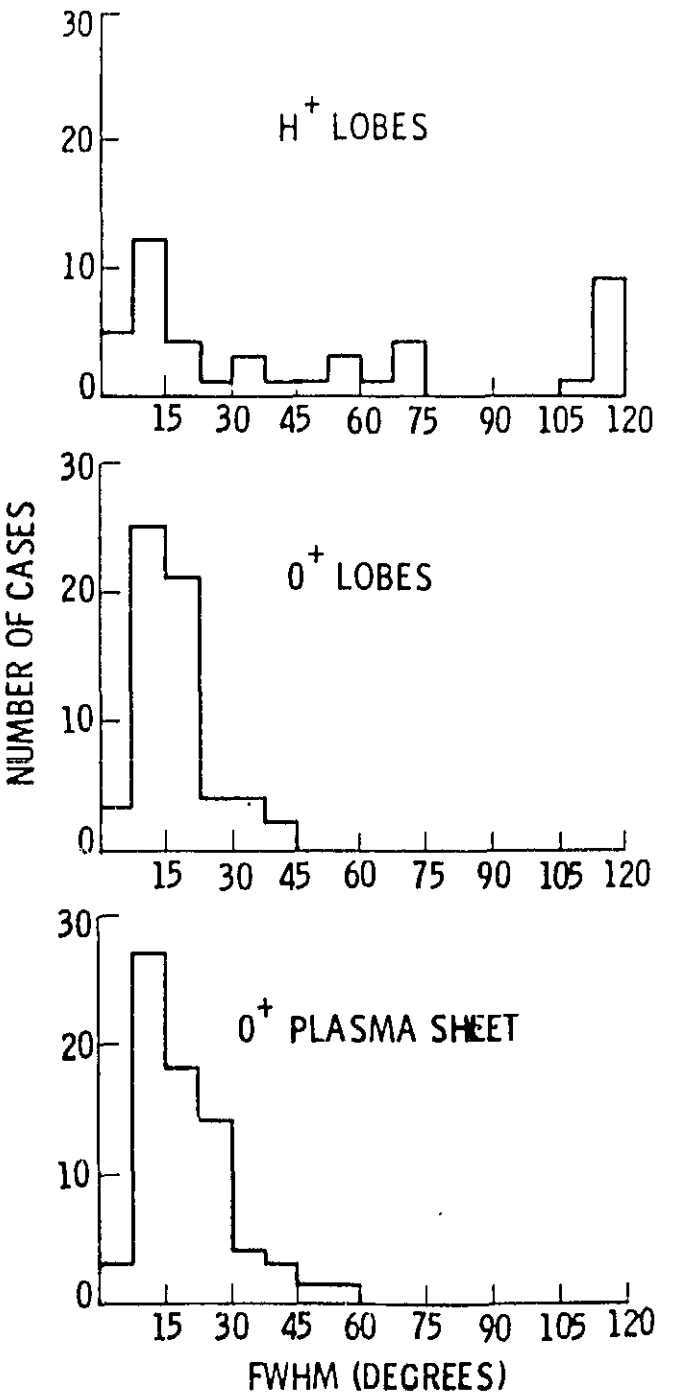

Figure 12. Distributions of ion streams with respect to the observed full widths at half maximum of their angular distributions (Ref. 27).

the H^+. The combination of higher intensity and higher frequency of occurrence (Table 2) means that the O^+ was clearly the dominant constituent of the tail lobe plasmas with E > 110 eV during the period of this study.

Table 2: STATISTICAL STUDY OF ION BEAMS IN THE MAGNETOTAIL

Ion	Location	Kp†	Samples	Frequency,%
H^+	lobes	lo	294	9.9 ± 1.8
		hi	249	11.6 ± 2.2
		all	543	10.7 ± 1.4
O^+	lobes	lo	294	9.9 ± 1.8
		hi	249	24.5 ± 3.1
		all	543	16.6 ± 1.7
O^+	plasma sheet	lo	250	10.4 ± 2.0
		hi	285	45.6 ± 4.0
		all	535	29.2 ± 2.3

†lo $\leq 3^+$, hi $\geq 4^-$

We know that the O^+ streams must be of ionospheric origin and we infer from the similarity of the gross properties of the O^+ and H^+ streams that they originate from the same source. We infer from these results that it is probable that both the O^+ and most of the H^+ streams in the central regions of the magnetotail are of ionospheric origin. Streams with the characteristics of the boundary layer or mantle, which are primarily of solar wind origin, were not found within the limited region and period of this study. This inference results in some modification of recent ideas about the formation of

the plasma sheet. Hardy et al. (Refs. 13, 28, 29) were able to detect the tail lobe streams with their electrostatic analyzer on the moon, but without mass discrimination they could not differentiate them from the boundary layer or plasma mantle streams. Their results were taken as evidence that the mantle plasmas could convect inward from the magnetopause to the plasma sheet at geocentric radial distances as low as 60 R_E, although as noted by Hardy et al (Ref. 28) and Crooker (Ref. 30), the magnitude of the typical crosstail field did not appear to be adequate to produce this effect.

Pilipp and Morfill (Ref. 31) used these results as the basis of their model in which the entire plasma sheet was produced by the inward convection of mantle plasma. The present results suggest that the polar cap ionosphere can be an additional source of ion streams which are eventually carried to the plasma sheet by the crosstail convection field. Other ionospheric streams are directly injected onto plasma sheet field lines. As seen in the previous section, especially during active times, these ionospheric ions can form an important, occasionally dominant, fraction of the plasma sheet.

Some additional insight into the nature of the mechanism that eventually thermalizes the magnetotail streams can be obtained from the apparent mass dependence of this process. On those occasions when both O^+ and H^+ streams are observed simultaneously the H^+ beams often exhibit a substantially broadened pitch angle distribution or a conical angular distribution characteristic of a high transverse to parallel temperature ratio while the simultaneously observed O^+ is in the form of a narrow, nearly field-aligned beam. An example of this on April 19, 1978 is shown in Figure 13. A similar example was presented in Figure 4 of Ref. 27. The high transverse temperature implied by these broad H^+ distributions must have been imparted by a local acceleration mechanism since any transverse energy acquired by the ions in the ionosphere would have been largely converted to parallel energy as they streamed into the weak magnetic fields of the magnetotail.

As seen in Figure 12 the initial statistical results also indicated that the H^+ distributions in the tail lobes were more likely than the O^+ to exhibit high transverse temperatures. These results are somewhat puzzling since the opposite effect was found by the S3-3 satellite in the auroral acceleration region. In the upflowing ion beams with keV energies observed at altitudes greater than ~ 5000 km, the O^+ angular distributions were found to be broader than the H^+ distributions and their energies were substantially higher (Ref.

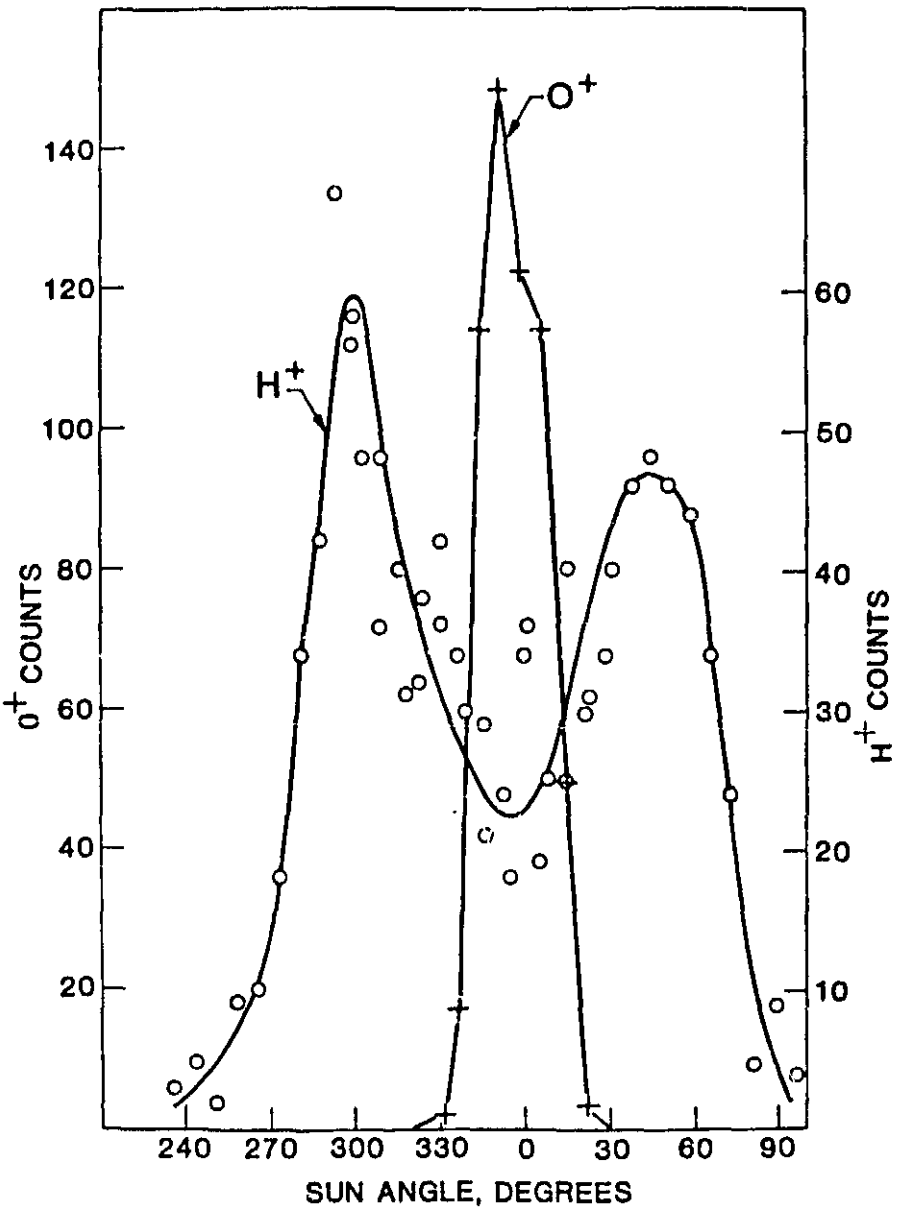

Figure 13. Angular distributions of 628 eV O^+ ions and 212 eV H^+ ions in a tail lobe stream on April 19, 1978 at 0500 UT. These are the energies corresponding to the peak response for the respective species.

9). This was taken to be the result of a mass dependent transverse acceleration mechanism which preferentially acted upon the O^+ component of the beams, both components of which had also been energized by quasistatic electric fields.

A possible explanation for this discrepancy may lie in the recent theoretical work of Ashour-Abdallah et al (Ref. 32). They have extended the analysis of Kindel and Kennel (Ref. 33) for the situation applicable to the auroral ionosphere in which the cold ionospheric electron population drifts relative to the ambient ionospheric ions, exciting ion cyclotron waves and transversely accelerating the ions. In a simulation study with an initial drifting electron Maxwellian, Ashour-Abdalla et al. (Ref. 32) showed that the oxygen waves grew to only small amplitudes because the hydrogen waves extracted most of the free energy from the electrons before the oxygen waves could grow. This was contrary to the above-mentioned energetic ion observations in the auroral region and they suggested that the dilemma could be resolved if the electron velocity distribution was maintained by the constant injection of fresh electrons, inhibiting the above-described saturation effects. In the absence of this saturation they found that oxygen wave growth and transverse oxygen ion acceleration dominated over that of hydrogen in agreement with the S3-3 observations. In the tail lobes, however, the situation is reversed. Here we have ion streams flowing through a cold ambient electron plasma. The same electron population may be in contact with the ion stream for an extended period and some type of saturation effect may occur, leading to the preferential transverse energization of the H^+ component. A detailed simulation study using the appropriate plasma parameters for the tail lobes will be required to resolve this question but it is an interesting possibility for the resolution of the apparent conflict between the low and high altitude ion observations.

4. SCIENTIFIC RESULTS FROM THE INNER MAGNETOSPHERE

An important problem in magnetospheric research for which ion mass spectrometer data are particularly relevant is the origin of the storm time ring current. The first direct measurements of the composition of the trapped ring current ions were made with the S3-3 satellite and showed that in the energy range from 0.5 to 16 keV/e O^+ was often of comparable intensity to H^+

(Ref. 34). This confirmed earlier inferences of the importance of the ionosphere as a source term for this plasma population (Ref. 35). Later, on the basis of more extensive measurements from the GEOS satellites, it was inferred that in the regions of the magnetosphere accessible from the GEOS orbits, the solar wind (characterized by He^{++}), and the ionosphere (characterized by O^{+}) gave, on average, comparable contributions to the storm time plasma in the energy range from 0.9 to 16 keV/e (Ref. 22). Because of its unique orbital characteristics, the ISEE satellite can provide important complementary information to these earlier data sets, allowing direct measurements of the radial dependence of the near equatorial plasma population.

From the first 16 months of the ISEE data, Lennartsson et al. (Ref. 36) selected ten magnetic storms with peak Dst $\lesssim -100$ γ for which data in the inner magnetosphere were acquired during the early main phase. The data set provided relatively complete coverage of the inner magnetosphere between about 2 and 15 R_E at all local times. The average densities of the various ionic constituents were computed over time intervals corresponding to a spacecraft motion of about 1 R_E in radial distance. This amounted to about 20 minutes at $R \sim 2$ R_E and to more than 1 hour at $R \sim 15$ R_E. The calculations assumed isotropic angular distributions and included energies in the range from 0.1 to 17 keV/e. The overall results are summarized in Figure 14. These histograms give the frequency of occurrence of different ion concentrations in all of the intervals studied without any discrimination with respect to radial distance or local time. The remaining fraction in each case consisted essentially entirely of H^{+}. In some cases only upper limits on the densities could be established because of background due to penetrating radiation or poor counting statistics. If each upper limit is treated as a real density then the solid histograms apply. If it is neglected then the dashed histograms apply. The actual frequency of occurrence lies somewhere between the two.

The most striking feature of Figure 14 is the apparent large and variable ionospheric component of the measured plasma. Since all of the O^{+}, almost all of the He^{+}, and some unknown fraction of the H^{+} is of ionospheric origin it is clear that the ionosphere is an important, perhaps dominant contributor to the plasma in the energy range of this study. On the other hand, if one considers that the solar wind typically contains ~ 25 times as much H^{+} as He^{++}, the high frequency of measurable He^{++} densities suggest that this source term is also important, in agreement with the GEOS result.

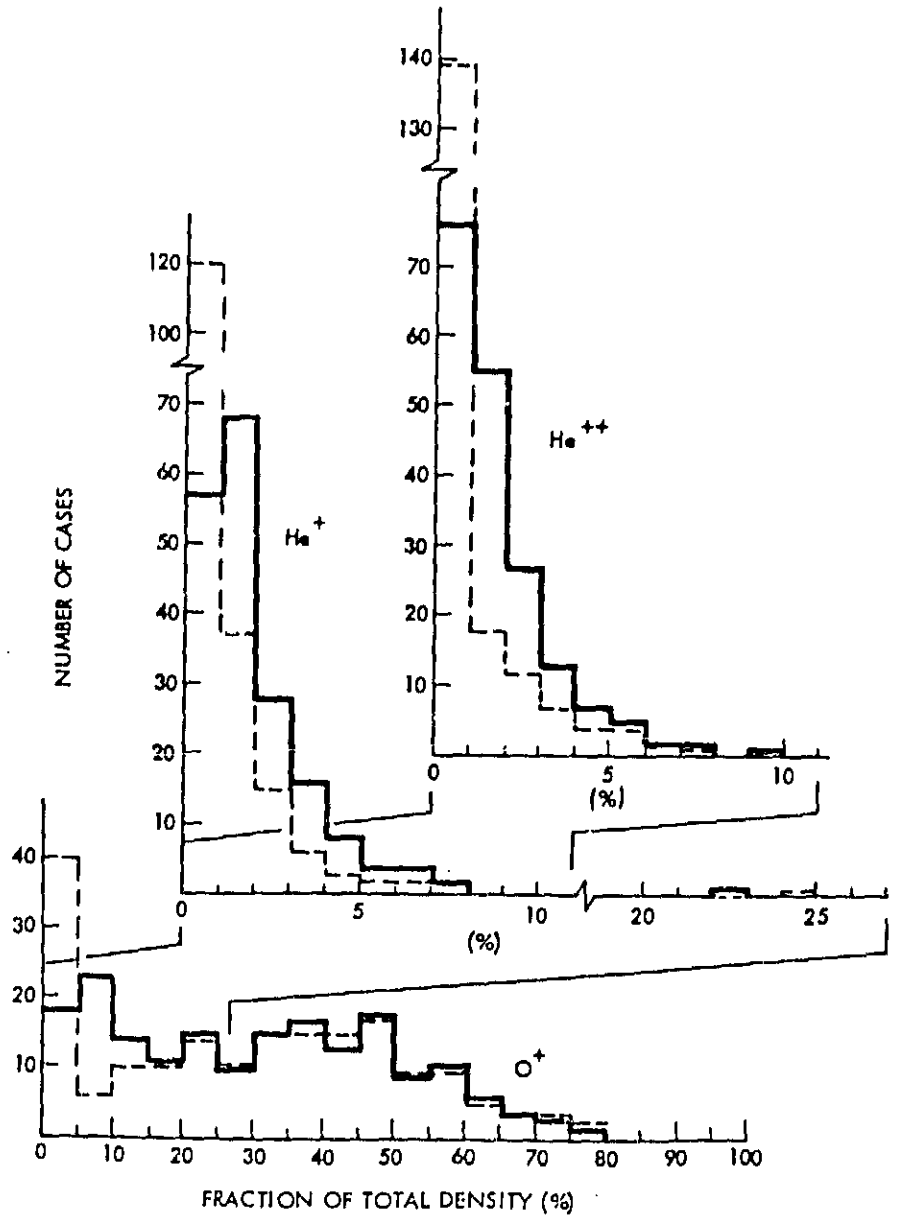

Figure 14. Distribution of fractional densities of O^+, He^+ and He^{++} in the inner magnetosphere (2-15 R_E geocentric distance) during magnetic storms (Ref. 36).

Some insight into the particle dynamics during these magnetic storms can be obtained by an examination of the detailed distribution functions. A commonly observed feature of these distributions was a "hole" in the few keV range. Some examples are given in Figure 15. This "hole" was most clearly seen in the dayside magnetosphere and occurred at an energy that varied with local time and radial distance and also varied to some extent from event to event. This is apparently the same feature as the "deep minimum" discussed by McIlwain (Ref. 38) in the energy flux spectrums taken by the geosynchronous satellite ATS-5. As reported by McIlwain, this flux minimum seems to be at a demarcation energy between ions (with low energy) that have drifted through the dawnside magnetosphere and ions (with higher energy) that have drifted through the dusk region. That is, the minimum corresponds to ions not yet arrived (due to slow drift close to the earth) or ions already lost (due to high loss rates close to the earth). The frequent occurence of this spectral feature suggests that much of the time the large scale drift motion of the particles can be described by almost constant magnetic moments, resulting in a relationship between the measured energy and spatial origin of the ions such as is illustrated in Figure 16. In this schematic diagram the phase space density is assumed to be measured at a fixed pitch angle (e.g. 90^{o}) and the ions are assumed to be injected at a fairly well defined radial distance and to preserve their magnetic moments while drifting sunward under the influence of a dawn-dusk electric field.

Some corroboration of this interpretation for the O^{+} fluxes measured by ISEE during the December 11, 1977, magnetic storm was presented by Lennartsson et al. (Ref. 37). Data from this event taken between 11.1 and 11.8 hours local time and at L values between 3 and 4 have been shown in Figure 15a. From similar spectrums taken during this entire dayside magnetospheric traversal Lennartsson et al. have plotted the location in energy of the deepest minimum in the O^{+} distribution as a function of geocentric distance (See Figure 17). The dashed curve shows the energy at which westward gradient B drift in the equatorial plane is exactly cancelled by eastward co-rotation convection (for 90^{o} pitch angle particles in a dipole field). The remarkable agreement provides strong support for the conclusion that the "hole" in the distribution function is the demarcation between low energy ions circling the earth in the eastward direction and high energy ions circling the earth westward.

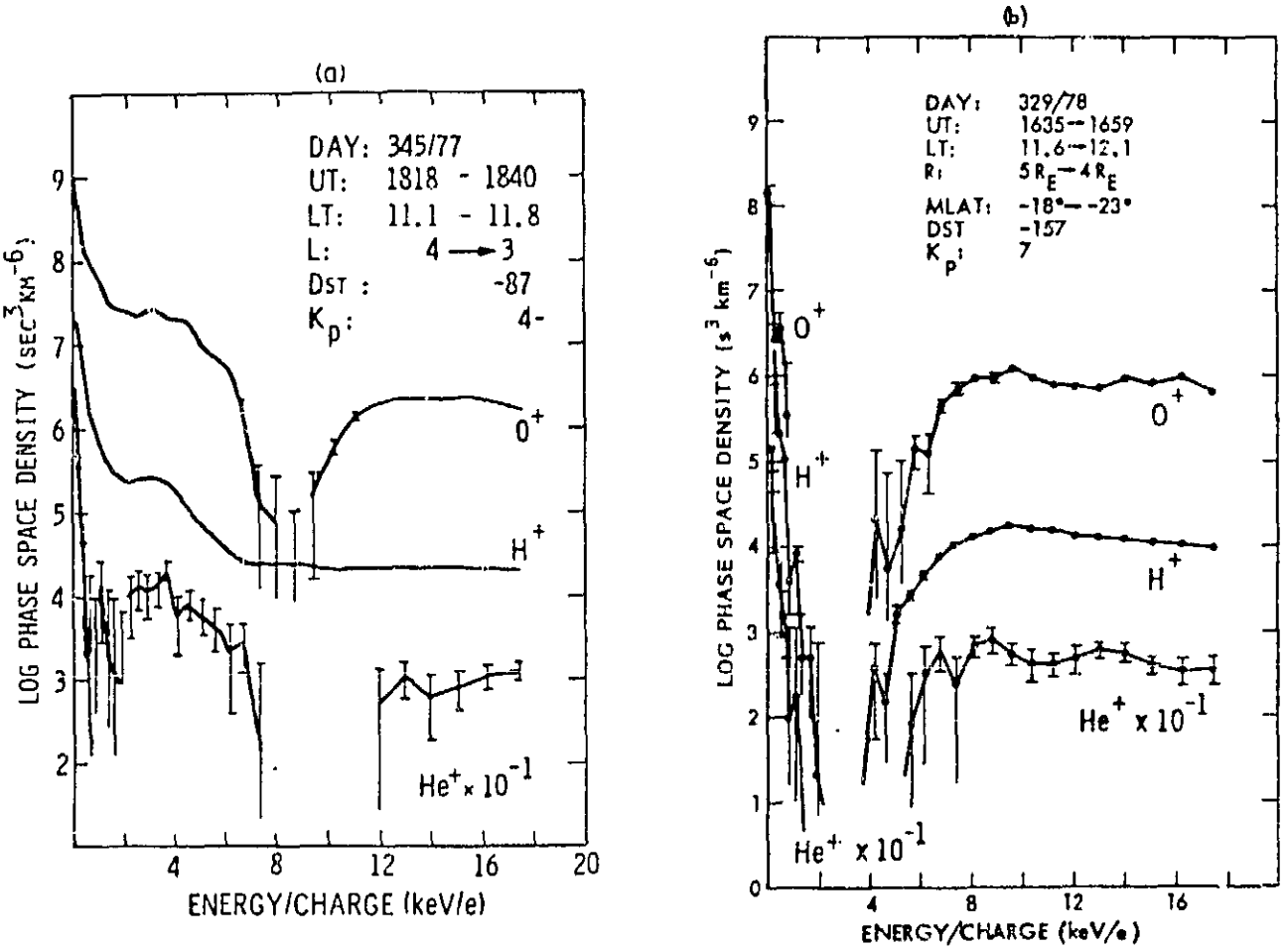

Figure 15. Phase space density distributions exhibiting a "hole" in the few keV range (Ref. 36 and 37).

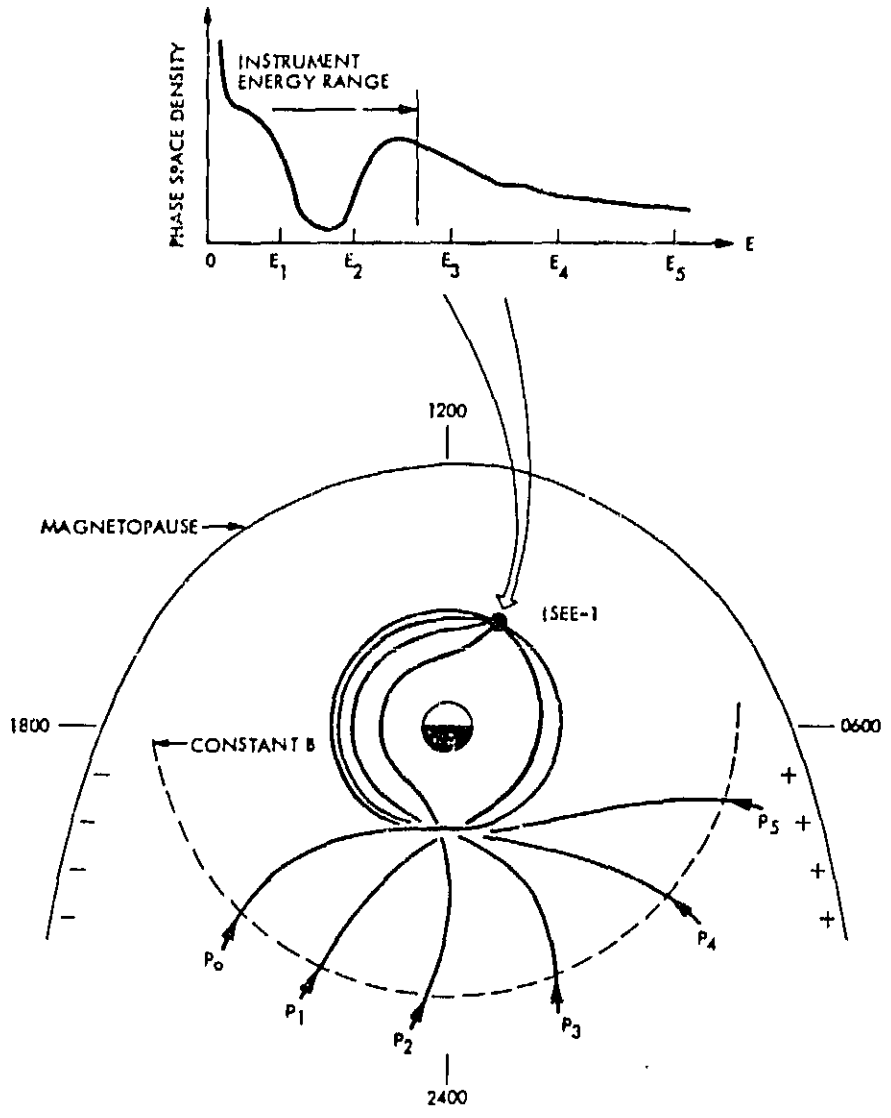

Figure 16. Schematic illustration of a relationship between measured energy and spatial origin of ions (Ref. 36).

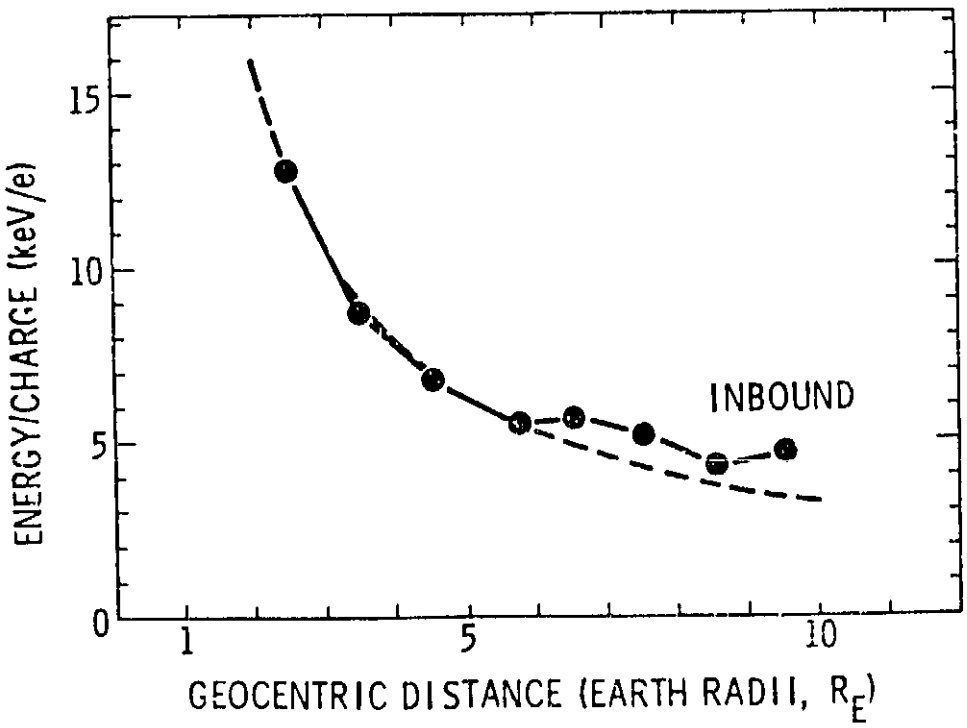

Figure 17. Energy at deepest minimum in phase space density distribution as a function of geocentric distance, for O^+ ions on December 11, 1977 (solid line) and energy at which co-rotation cancels gradient B drift (dashed line).

The detailed motion of the ions in any individual event will of course depend on the spatial structure and time dependence of the electric field, but to the extent that the model represented by Figure 16 is qualitatively valid, in some average sense, for the 10 magnetic storms which contributed to the data set discussed above, we have the opportunity to use this data to investigate the important portion of the ring current distribution function that is above the energy range accessible to the present generation of ion mass spectrometers. As shown by Smith and Hoffman (Ref. 39) and Williams (Ref. 40) the portion of the spectrum in the 50-100 keV range dominates the energy density of the trapped particles in the L $\sim$ 3-4 region of the magnetosphere where most of the ring current energy is concentrated. By studying these ions at high altitudes in the predawn local time sector (P4 and P5 in Figure 16) we can investigate their composition at a location in the magnetosphere where they are still within the energy range of the ISEE spectrometer.

This has been done by dividing the data represented by the histograms in Figure 14 into two subgroups depending on their local time, and plotting them as a function of geocentric radial distance. Figure 18 shows the results for the O^+ to H^+ number density ratios. Samples taken in the 0100 to 0600 LT sector are indicated as triangles and the remaining data are represented by circles. Upper limits are marked by open symbols. The solid and dashed lines are the medians of triangular and circular data symbols respectively. One sees in Figure 18 that the largest O^+/H^+ ratios (near unity) are found at low geocentric distances. Despite the large variation in individual ratios, one can see a significant difference in composition between the high altitude, predawn data and the high altitude data in the remaining local time region. This is shown more clearly by the two histograms on the right hand ordinate. These show the total number of points (solid and open) in certain vertical bins for $R > 7\ R_E$. The solid histograms corresponds to the 0100 - 0600 LT sector and the dashed histogram corresponds to 0600 - 0100 LT. These results suggest that the plasma which will later become the high energy portion of the ring current spectrum have a significantly reduced oxygen to hydrogen ratio relative to the plasma in other sectors.

A plot of the He^{++}/H^+ density ratios in the same format as Figure 18 is shown in Figure 19. The two medians refer only to the solid data points in this figure. These ratios do not show a clearly significant radial dependence, but only limiting values are available at low geocentric distances

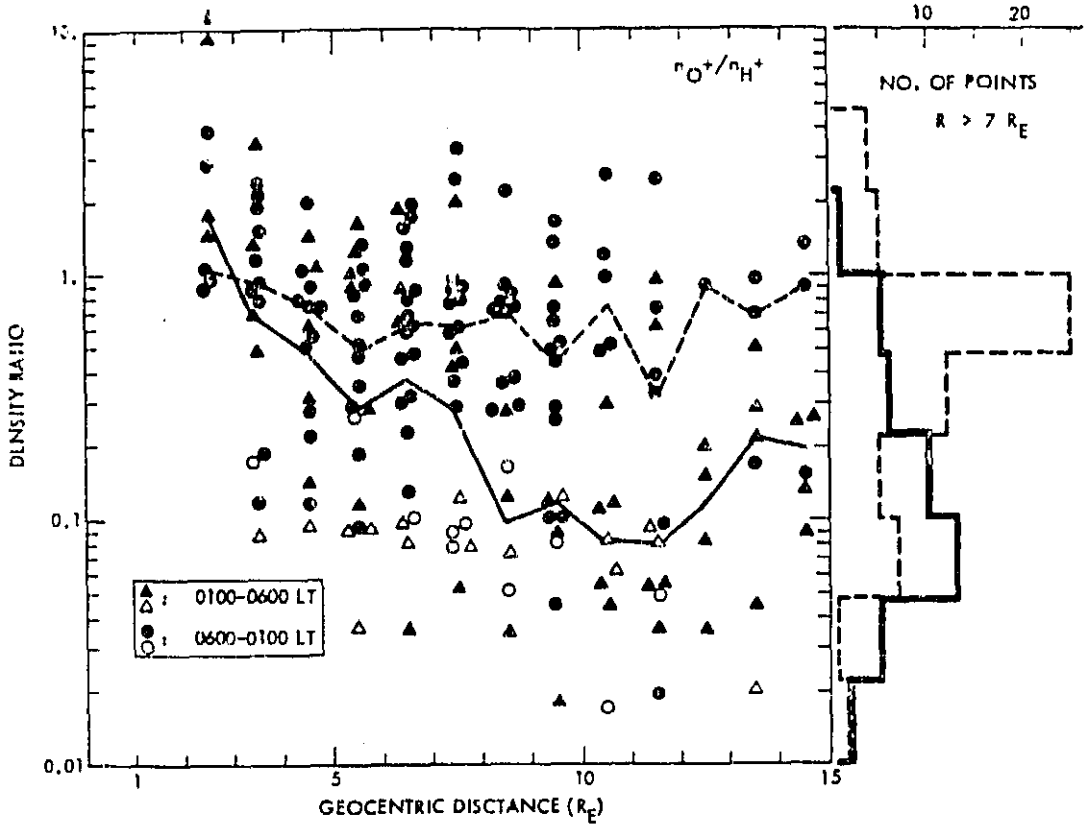

Figure 18. O^+/H^+ density ratios during storms as a function of geocentric distance. Upper limits are indicated by open symbols. Triangles represent data in the 0100 to 0600 LT sector and circles represent data in the 0600 to 0100 LT sector. The two histograms to the right show the total number of points in the indicated vertical bins for R > 7 R_E. The solid histrogram corresponds to the 0100 to 0600 LT data and the dashed histogram to the 0600 to 0100 LT data (Ref. 36).

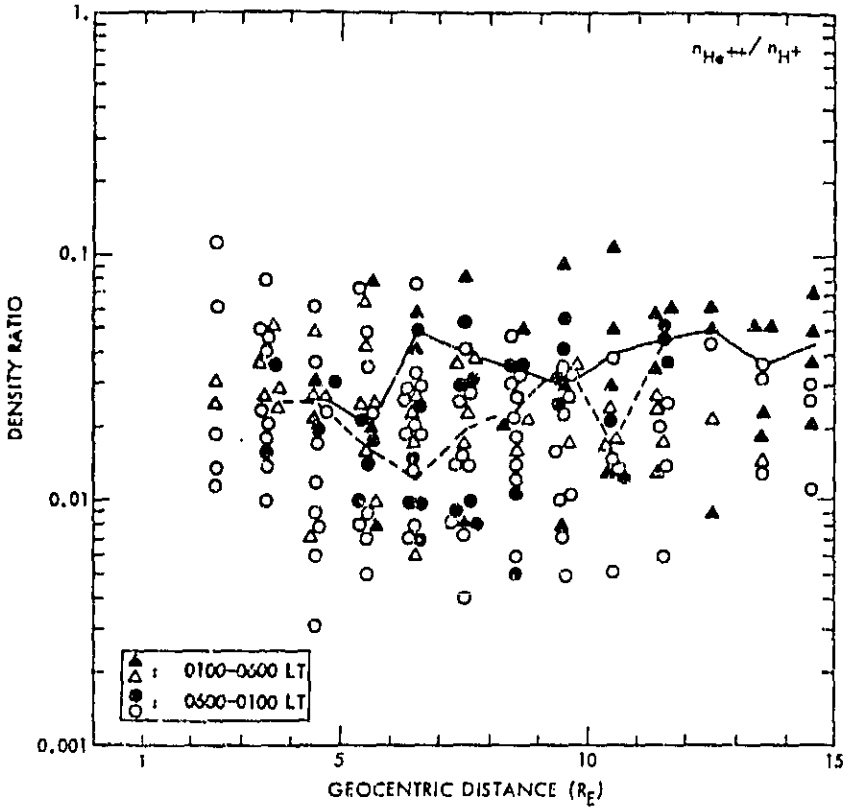

Figure 19. He^{++}/H^{+} density ratios in the same format as figure 18 (Ref. 36).

because of background effects on the He^{++}. Although these results are less definitive than those in Figure 18 it is probable that the data at large radial distances ($R > 7\ R_E$) in the 0100 to 0600 LT sector is richer in He^{++} than the corresponding data at other local times. Taken together these results suggest that the solar wind is a more important contributor to the ring current energy than the available data in the energy range below $\sim$ 17 keV/e would indicate. However, as is apparent in Figures 18 and 19 the ratios are highly variable and the differences between their average values in the two local time sectors are not dramatic and do not suggest that the solar wind is always the dominant source of ions in the high energy ring current.

A study by Lennartsson and Sharp (Ref. 41) has allowed for a comparison of the ion composition in the near equatorial magnetosphere during quiet and disturbed conditions. Data acquired during some 24 traversals of the magnetosphere at different local times and $R \lesssim 15\ R_E$ during very quiet periods were compared with the above described data taken primarily during the early main phase of magnetic storms. Figures 20, 21, and 22 show the average density ratios of the various ionic constituents in the energy range 0.1 to 17 keV/e as a function of L for the two data sets.

Looking first at the quiet time results, the most striking feature is the rapid rise in the He^+/H^+ and O^+/H^+ ratios at low L values. This is qualitatively consistent with expectations from charge exchange since H^+ has by far the shortest lifetime of the three species. At 5 keV for example $\tau(H^+):\tau(O^+):\tau(He^+) \approx 1:7:50$ (Ref. 42). However, as discussed by Lennartsson and Sharp (Ref. 41), the results are not quantitatively consistent with these estimated charge exchange lifetimes and the expected ion drift paths. These lead to the prediction of much higher O^+/H^+ and He^+/H^+ ratios than those observed, particularly at $L \lesssim 4$. The dominance of H^+ at $L > 5$ in the quiet time data shows that charge exchange is not the primary element in establishing the ionic composition in that range. Additionally, the similarity in the shapes of the quiet time O^+/H^+ and He^+/H^+ curves in Figures 20 and 21 indicates that the O^+/He^+ ratio remains at an almost constant value ($\sim$ 5) over the altitude range of the study. This generalization can even be extended to include the magnetotail data discussed earlier. The quiet time data in Table 1 were acquired at a mean geocentric radial distance of 16.3 R_E (variance = 3.0 R_E) and indicate an O^+/He^+ density ratio of 5.6 ± 1.1. The approximate constancy of this ratio over such an extended altitude range suggests that

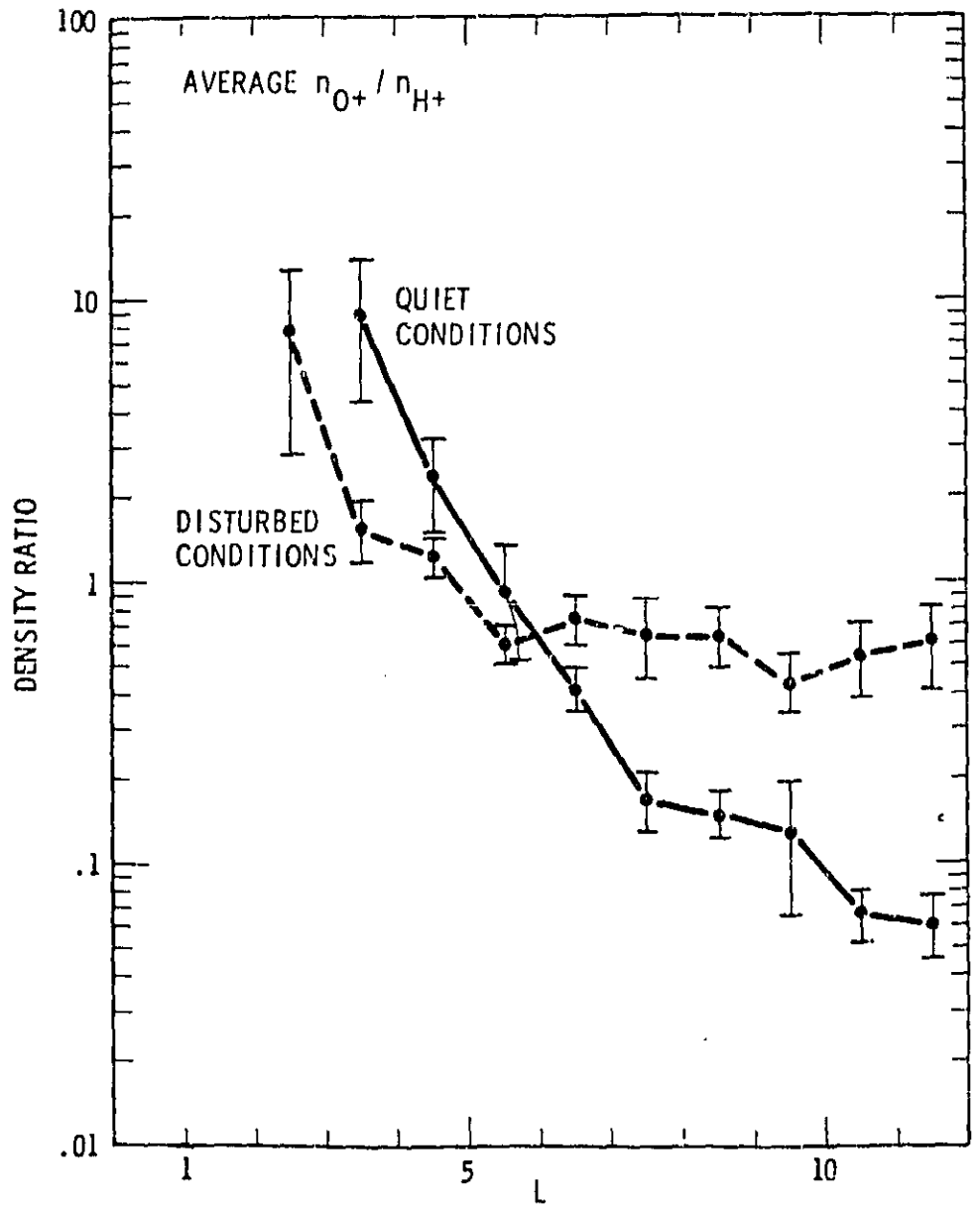

Figure 20. Average O^+/H^+ density ratios as a function of L for quiet and disturbed conditions (Ref. 41).

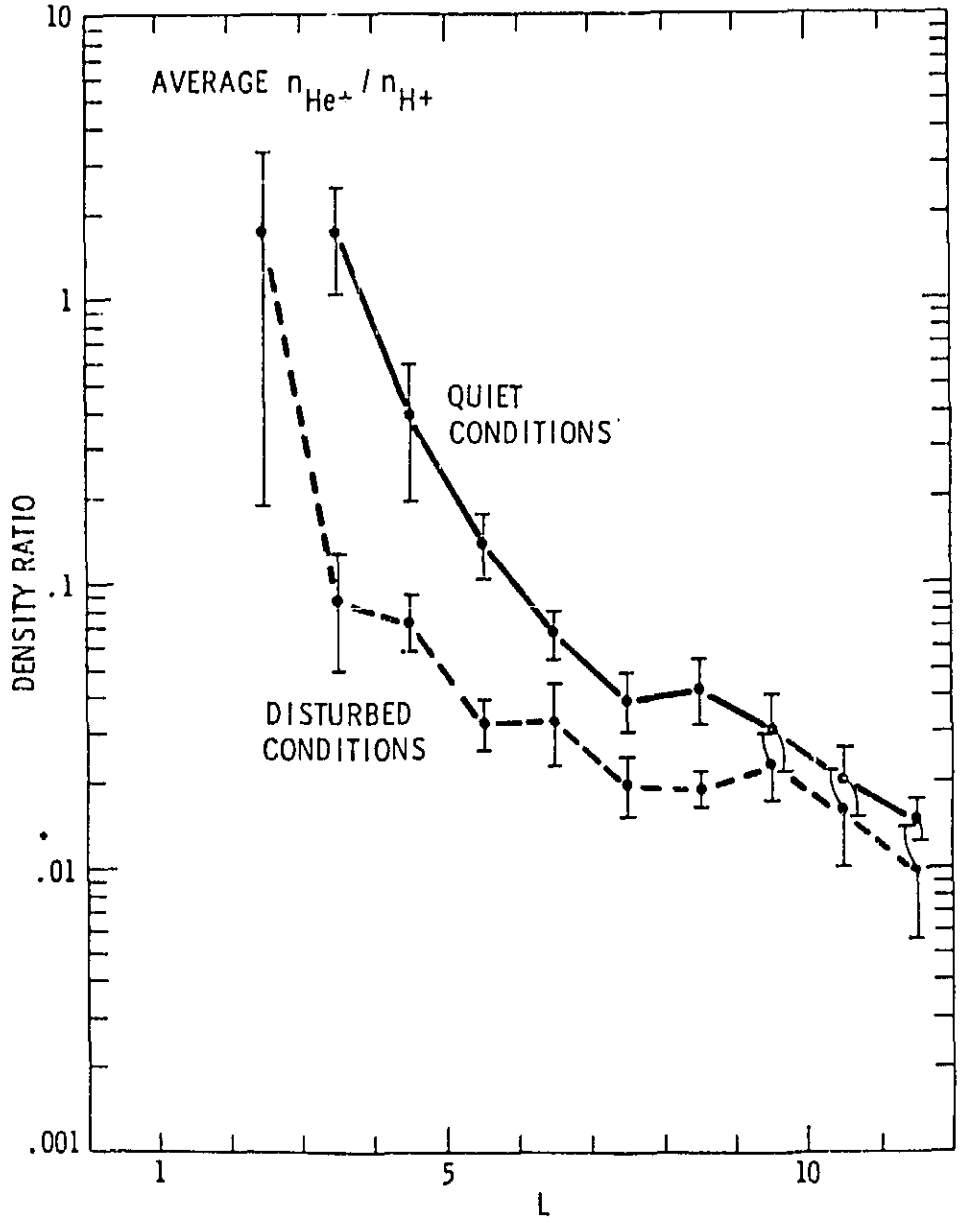

Figure 21. Average He^+/H^+ density ratios as a function of L for quiet and disturbed conditions (Ref. 41).

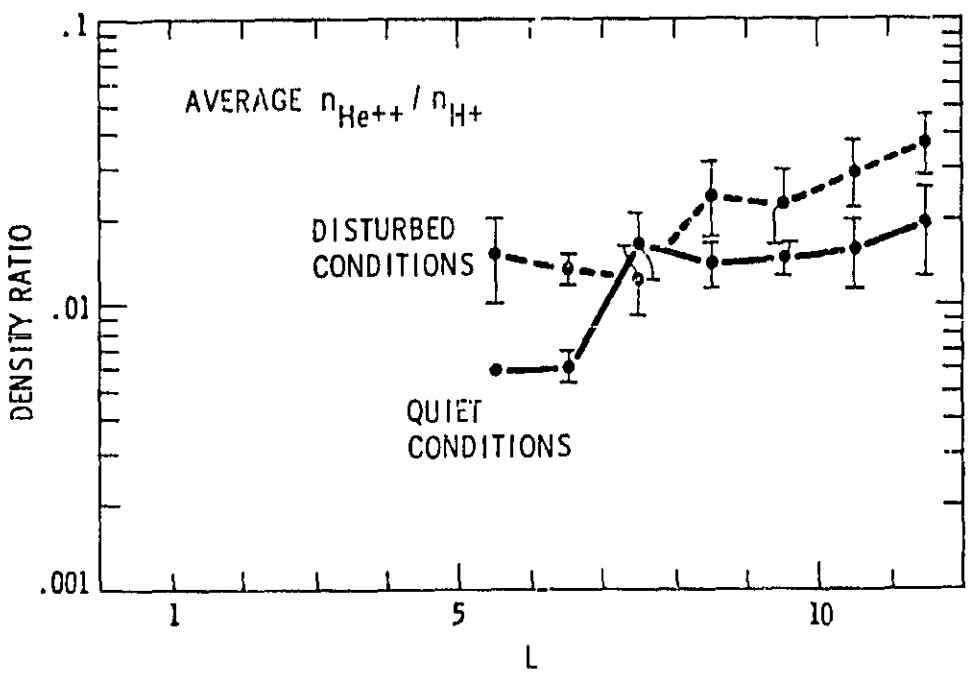

Figure 22. Average He^{++}/H^{+} density ratios as a function of L for quiet and disturbed conditions (Ref. 41).

mass dependent loss processes such as charge exchange are not substantially affecting these two ion species as they convect inward.

A more explicit illustration of the evolution of ring current ion populations during a single magnetic storm is provided by Figures 23 and 24. These figures are taken from a study that is not yet completed. The data are from two successive orbits of the ISEE-1 spacecraft, one intersecting the dayside near-equatorial magnetosphere shortly after the peak DST of a major magnetic storm, as illustrated at the top of each figure (label 1), and the next orbit intersecting the same general region during the decay phase of the storm, 57 hours later (label 2). The data from the first orbit, mean energies in the upper panel and number densities in the lower panel, are plotted with a fine dashed line as functions of the dipole L parameter (in units of earth radii). The data have been averaged over segments of L as indicated by the horizontal portions of the curves. Data on H^+ ions are shown in Figure 23 and data on O^+ ions, and some data on He^+ ions, are shown in Figure 24. Data from the second orbit are plotted with a heavy solid line, including error bars due to the poorer counting statistics (the error bars from the first orbit are generally too small to show). The measured fluxes have been averaged over the pitch-angle range 50^o - 120^o, which is the maximum range covered by the instrument on these occasions. The corresponding energy distributions have been integrated from 1 to 16 keV to yield the mean energies and densities. Despite the limited pitch-angle coverage here the number densities have been normalized to the full unit sphere (4π) for easier comparison with the data covering larger angles.

The heavy dashed lines in Figures 23 and 24 show predictions for the second orbit based on data from the first orbit and theoretical charge exchange life times taken from Ref. 43. The theoretical charge exchange life times, which are primarily defined by charged exchange with neutral hydrogen, depend on the scale height of the neutral atmosphere which varies somewhat depending on the density and temperature at the exobase (Ref. 43). To be able to make some quantitative comparisons with our data we chose the exobase density and temperature from within their normal range of variability so as to give exact agreement between the measured and predicted H^+ density between L = 6 and L = 7 (in the vicinity of the geosynchronous orbit). The predictions are made under the assumption that the ions remain on constant L-shells after the storm injection on Dec 11, an assumption that is strongly questionable, of

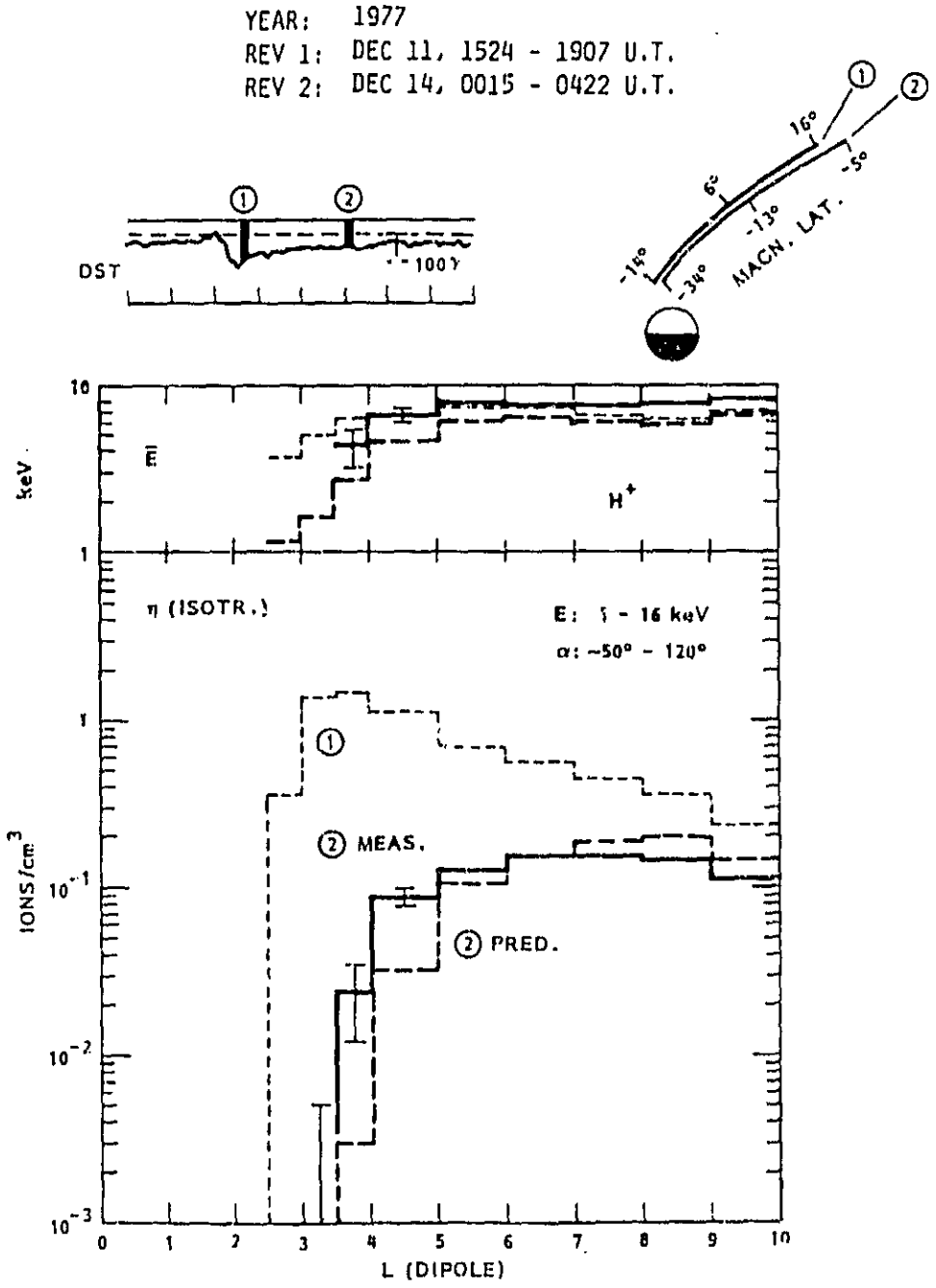

Figure 23. H^+ energies and densities measured during two successive traversal of the dayside magnetosphere during a major magnetic storm, along with theoretical predictions for the second traversal based on charge exchange decay of the measured ions from the first traversal (see text).

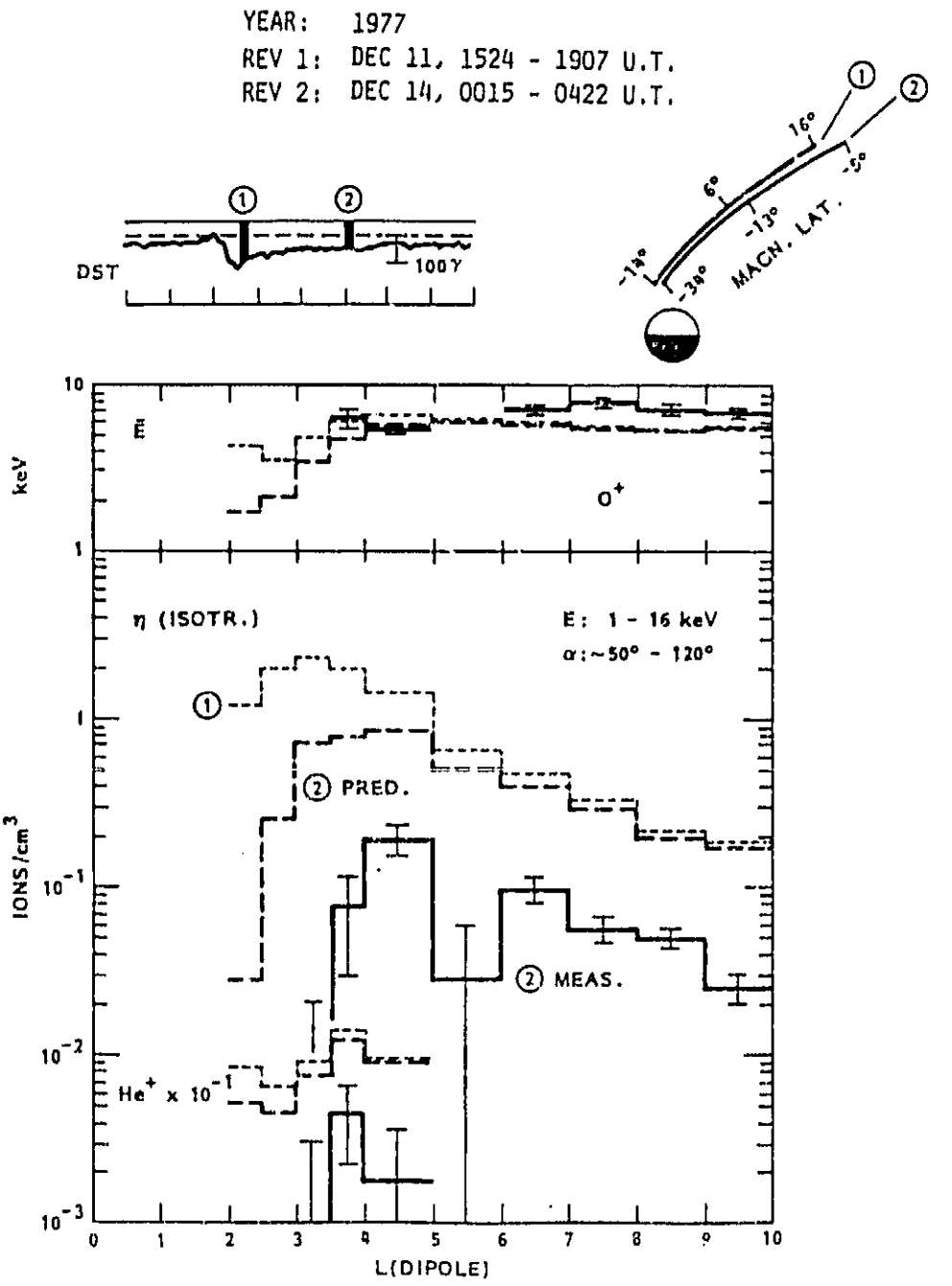

Figure 24. Same as Figure 23 but showing data for the O^+ (and some data for the He^+).

course, but is nevertheless often made in the literature in order to demonstrate the effects of charge exchange.

A comparison between the measured and predicted H^+ densities during the second orbit in Figure 23 shows a discrepancy between the L-profiles of the two sets of densities, but the maximum distance between the two profiles is nevertheless reduced by our normalizing the theoretical H^+ densities to the measured H^+ densities in the middle of the L-range. However, if we compare the predicted and measured densities of O^+ ions (and He^+ ions) in Figure 24 we find a discrepancy of one order of magnitude or more throughout the L-range. The predicted O^+ densities are a consequence of our normalizing the neutral atmosphere parameters so as to give reasonable agreement for the H^+. If instead we normalize these parameters to give better agreement for the O^+ we get, of course, a correspondingly worse agreement for the H^+. As a matter of fact, if we select the atmospheric parameters to give good agreement for the O^+ at L ~ 4-5, for example, the predicted H^+ density in that same L-range will be reduced by 4 orders of magnitude. In other words, it is impossible to select the atmospheric parameters to give reasonably good agreement for both the H^+ and the O^+ at the same time during this particular event.

Taken together, these results suggest that models based primarily on the charge exchange decay of static trapped populations of ions are not likely to be successful in explaining the detailed evolution of the ring current (Refs. 42, 44, and 45). Instead, the results seem to require continuous injection, even during periods of extended quiet, or transport times which are not long compared to the charge exchange life times of the heavier ion species, or additional decay processes other than charge exchange, or a combination of all these processes.

Although the charge exchange with neutral hydrogen is undoubtedly an important loss process for ring current ions at low altitude it may have rather negligible effects at high altitudes. Returning to Figure 20 we take notice of the crossover in the O^+/H^+ ratios from quiet and disturbed times at L ~ 5-6. Inside of L = 5 the O^+/H^+ ratio is highest during quiet conditions, on the average, which may well be due, at least to a significant extent, to the more rapid charge exchange of H^+ ions. However, at L > 6 the O^+/H^+ ratio is highest during disturbed conditions which may reflect the ion injection processes rather than the loss processes. It may seem reasonable therefore to assume that charge exchange is a negligible process here and that the major

loss of plasma from these altitudes is due to convective motion and gradient-B (and curvature) drift. Since these latter processes are basically independent of the ion species (given the energy-per-charge) we may be able to trace the observed species-dependent features in our data from $L \geq 5$ to the ion composition of the plasma sources. In particular, the observed variations in the O^+ and He^{++} densities may directly reflect varying contributions from the terrestrial source and from the solar wind source, respectively.

With this approach in mind we have used the average ion density ratios in Figures 20-22, along with the statistical error bars, to infer the relative contributions of ions from the solar wind and the earth's ionosphere during quiet and disturbed conditions in the altitude range $5 < L < 12$ (Ref. 46). The resulting numbers, which correspond to the energy range 0.1 - 17 keV/e, are displayed in Table 3. The upper panel contains our estimates of the average O^+/H^+ ratio in the purely ionospheric plasma contribution ($H^+ = H^+_1$) and, for comparison, the typical O^+/H^+ flux ratios of upflowing ion beams observed by the S3-3 spacecraft over the polar regions of the ionosphere and covering the energy range 0.5 - 16 keV/e (Ref. 47). The lower panel contains our estimates of what fraction of the total ion density is of ionospheric origin.

In order to obtain these numbers we have assumed that all of the O^+ and He^+ ions and an unknown part of the H^+ ions are of ionospheric origin, whereas all of the He^{++} ions and the remaining part of the H^+ ions are of solar wind origin. Furthermore, we have assumed that the He^{++}/H^+ density ratio in the solar wind is equal to 1/22, which appears to be in reasonable agreement with published data. The main conclusion that can be drawn from this table is that the ionospheric contribution to the energetic ($\leq$ 17 keV/e) ion population inside of $L = 12$ is quite substantial and may dominate, even as a rule, during major magnetic storms. A more detailed discussion of these numbers and of the assumptions is given in Ref. 44.

Another area of magnetospheric research in which composition measurements are of importance is the study of geomagnetic micropulsations. Magnetic pulsations in the 10 to 600 second period range (Pc 3-5) are a common phenomena in the dayside magnetosphere. They are generally thought to be the result of standing wave resonant field line oscillations. To compare the observed periods with theory it is necessary to know the mass density and thus the composition of the ambient plasma. Composition data have not generally been available and

theoretically predicted resonance periods based on the assumption of a pure proton-electron plasma have often been in disagreement with observations.

Table 3: RELATIVE CONTRIBUTION OF IONOSPHERIC IONS

	ISEE							S3-3
L =	5	6	7	8	9	10	11	12	5000 - 8000 km alt.
(O^+/H^+_1)								
quiet	1.0	.47 ±.09	.27 ±.08	.22 ±.05	.19 ±.10	.10 ±.03	.10 ±.04		0.1-0.4
storms	.82 ±.21	1.1 ±0.2	1.1 ±0.4	1.5 ±0.7	.83 ±.28	1.7 ±1.1	3.6 ±4.9		0.7-2.1
f_1								
quiet	.86	.80 ±.03	.33 ±.18	.44 ±.10	.38 ±.09	.29 ±.20	.16 ±.30		
storms	.78 ±.08	.82 ±.03	.76 ±.09	.64 ±.11	.66 ±.09	.55 ±.12	.47 ±.15		

A detailed analysis of a set of long period ULF pulsations which were observed by the ISEE magnetometers on December 11, 1977 has been conducted by Singer et al. (Ref. 48)). During the period of interest there was a substantial fraction of O^+ in the measured plasma resulting in a mass density five to nine times greater than would have been computed on the basis of a pure proton-electron plasma. The expected wave periods under these circumstances are two to three times longer than they would have been if H^+ were the only ion present. The observed periods were in good agreement with theoretical predictions for a second harmonic standing wave oscillation. (The fundamental magnetic field oscillation is thought to have a node at the magnetic equator near where the data were acquired). It is concluded that composition data are a requirement for any serious quantitative intercomparisons of measurements with theory.

5. SCIENTIFIC RESULTS FROM THE MAGNETOSPHERIC BOUNDARY REGIONS

Measurements of the relative H^+ and He^{++} distributions in the magnetosheath can provide insight into possible mass and charge dependent process that may occur in the bow shock and magnetosheath. Such distributions were examined by Peterson et al. (Ref. 49) on eight magnetosheath traversals in the 0800-1100 local time range. Moments of the distributions functions were calculated and showed that bulk velocities of the two species, averaged over several minute intervals, were equal within experimental uncertainities. Both species exhibited temperature anisotropies with $T_\perp > T_{||}$ and both had high energy tails, i.e. excess flux at high energies relative to a best fit Maxwellian. There was a remarkable difference in the distribution functions of the two species at low thermal speeds in the form of a lack of He^{++} ions relative to H^+ ions in this portion of the spectrum. An example of this effect is shown in Figure 25. A similar effect was observed on all 8 traversals. A possible mechanism which could lead to such a phenomena was described by Peterson et al. (Ref. 49) as follows:

Electric potentials in the bow shock are determined by the energy of the dominant solar wind ion (H^+). Minor heavy ions species, with high mass to charge ratios and high energies, pass through the shock front with only limited changes in kinetic energy. Behind the shock front irregular magnetic fields randomize velocity directions of the minor heavy ions but have little effect on kinetic energy in the center of mass coordinate frame. The result would be a heavy ion distribution function having the form of a hollow shell moving with the same bulk speed as the primary component (H^+).

Peterson et al. (Ref. 50) have examined the composition data in nine cases when the ISEE satellite traversed the dayside magnetospheric boundary regions in the vicinity of the subsolar point for evidence of ions of ionospheric origin. The analysis was hampered by the relatively long cycle time of the spectrometer but the overall results provided convincing evidence that He^+ and O^+ ions with low flux intensities and keV energies can be found in the boundary layer, the magnetopause and the magnetosheath.

These data confirm earlier inferences based on the energy spectrums that magnetospheric particles can penetrate the magnetopause and contribute to the magnetosheath population (Refs. 51 and 52). The mass spectrometer results also suggested that the terrestrial contribution to the boundary layer ion fluxes

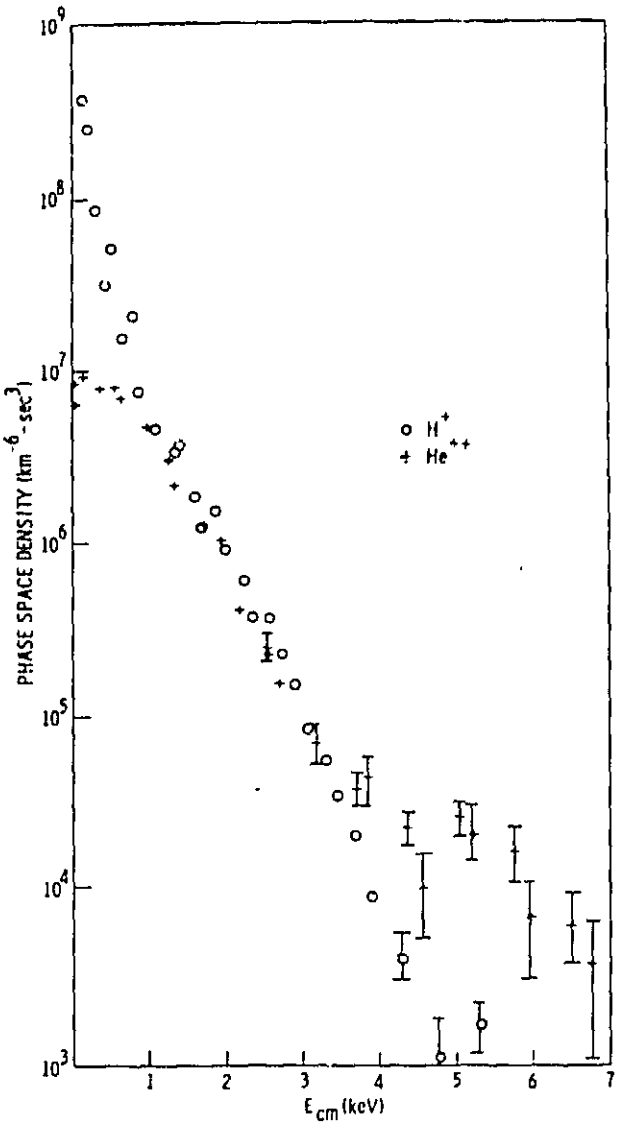

Figure 25. Phase space densities in the magnetosheath averaged over a 60° interval centered on the bulk flow direction and plotted against total energy in the center of mass frame. The data were acquired on 19 November, 1977 between 2330-2359 UT when ISEE was located between 13.7 and 13.2 R_E at ~ 0955 local time (Ref. 49).

might have had a different composition in the subsolar region than was typical of the boundary layer plasmas on the flanks of the magnetosphere. Preliminary results indicated that He^+ is most often dominant over O^+ in the subsolar region while O^+ is typically dominant on the flanks. This may be the signature of the process proposed by Freeman et al. (Ref. 53) in which plasmaspheric plasma, which typically is rich in He^+, is detached from the plasmapause and convected to the dayside magnetopause by the magnetospheric electric field. The He^+ ions could then become accelerated, mixed with the magnetosheath plasma, and injected into the plasma sheet in the magnetotail as discussed in the previous section.

The predominance of He^+ over O^+ is a relatively rare finding in the energetic plasma observations with the ion mass spectrometers on the several satellites that have probed throughout the magnetosphere. Except perhaps for the inner ring current during the late recovery phase of magnetic storms when charge exchange losses become important (Ref. 54) O^+ is generally dominant over He^+. Therefore, as discussed by Young (Ref. 55) the Freeman et al. mechanism is not likely to be a major source of energetic magnetospheric plasma. The ionospheric processes ocurring in the auroral acceleration region in which O^+ is strongly favored over He^+, seem to be the principal contributor of terrestrial ions to the magnetosphere.

6. NEW TECHNOLOGY

The analysis of data from the ISEE-1 Plasma Composition Experiment has been carried out with conventional tools and methods and has not lead to the development of new technology. The raw data from the instrument have the same basic form that has been utilized with electrostatic particle analyzers for decades, namely a number of particle counts per unit time and unit volume of particle velocity space. The only fundamental difference between these data and earlier particle data lies in the selection of particles by mass per charge. Our knowledge about the ion mass has so far been utilized for scientific purposes only and no technological application has yet been discovered.

7. CONCLUSIONS

During its approximately 4 1/2 years of operation (until March 20, 1982) the Plasma Composition Experiment on ISEE-1 gathered a very large and in most respects entirely unique set of data on the ion populations with energies in the 0.1-17 keV/e range. Due to the orbital characteristics of ISEE-1 data have been obtained in regions of space where mass spectrometers have never been flown before and may not be flown again in the foreseeable future, at least not before the OPEN project materializes.

Possibly the most significant results from the Plasma Composition Experiment so far relate to the energetic O^+ of ionospheric origin. The existence of energetic O^+ in the magnetosphere had already been established before the launch of ISEE-1, but the results from ISEE-1 have clearly demonstrated the pervasive nature of the O^+ both in terms of spatial distribution and velocity distribution. Many of the observed properties of the O^+ are beyond description by traditional theories of plasma circulation in the magnetosphere and will have a profound impact on future theories.

The results from the Plasma Composition Experiment have shown that the O^+ commonly contributes more than half of the ions with energies in the 0.1 - 17 keV/e range at $L < 5$, as illustrated in Figure 20, and is often the major component also at larger distances, especially during geomagnetically disturbed conditions (e.g. Refs. 16, 36, and 41). Much of the energetic O^+ ($\gtrsim$ a few keV) found at low L is consistent with the traditional picture of inward convection of ions from the plasma sheet (Figures 15-17) but a significant portion at energies of $\lesssim$ 1 keV appears to require a local source at low L. The same is true for the H^+ and the He^+ components as well (Ref. 41).

A very significant aspect of the ISEE-1 data from low L is the fact that the quiet-time ring current ion population with energies below 17 keV/e is dominated by the O^+ and not by the He^+, as previously postulated in the literature on the grounds that the He^+ has an exceptionally large charge exchange life time (Ref. 41). This is one of several aspects of the ISEE-1 data that raise questions about the relative importance of charge exchange in the general circulation of energetic plasma throughout the inner magnetosphere.

While the energy range 0.1-17 keV/e is insufficient to cover the bulk of the ring current ions it is generally sufficient to cover most of the plasma sheet ions, which are believed to be the main source of ring current ions.

Although the plasma sheet appears to be dominated by ions of solar wind origin (He^{++} and most of the H^{+}) during magnetically quiet conditions, in accordance with traditional belief, it does have a significant population of O^{+} most of the time and can be dominated, at least locally, by the O^{+} during active conditions. (Figures 4, 5, and 8). As a logical consequence of the traditional picture of plasma circulation one might therefore expect to find substantial numbers of O^{+} ions at all energies in the ring current.

Other regions accessible to ISEE-1 include the tail lobes (Ref. 27), the magnetopause boundary layers (Ref. 50), the magnetosheath (Ref. 49), and the solar wind (Ref. 6). A rather surprising result of the study by Sharp et al. (Table 2) is that the O^{+} dominates the tenuous tail lobe plasma with energies above 100 eV. In this region the O^{+} usually appears in the form of collimated streams flowing tailward with energies of a few hundred eV or less. Ionospheric O^{+} (and He^{+}) was also found in the magnetopause boundary layers and the magnetosheath (Ref. 50), but only in relatively small numbers. The fact that O^{+} exists at all near the subsolar magnetopause and in the magnetosheath is perhaps less significant than the fact that it is relatively rare there, since the conventional picture of plasma circulation would predict that the large amounts of O^{+} in the dayside magnetosphere would also show up in these outer regions.

In all regions where the O^{+} has been observed by the ISEE-1 instrument it has energies and magnetic moments that are vastly larger than those of the source population in the ionosphere. The O^{+} data, more than any other data, have made us realize that non-adiabatic acceleration of ions transverse to the magnetic field is a very fundamental process in the magnetospheric plasmas. This presents a serious challenge to existing theories of magnetospheric particle dynamics and may prove to be a milestone in space plasma exploration.

It appears in restrospect as though the "dramatic" character of the ISEE-1 observations of O^{+} ions may have been partly due to a fortuitous timing of the experiment. In the years following the launch of the ISEE spacecraft it has been discovered that the number of energetic O^{+} ions in the magnetosphere not only increases temporarily with increasing geomagentic activity but, on a timescale of months and years, also increases with increasing solar cycle activity on the surface of the sun, regardless of the level of geomagnetic activity. This discovery was made in data from the European GEOS-1 and -2 spacecraft (Ref. 20) but the correlation has been confirmed by the ISEE-1 data (Ref. 56). The physical mechanism for this solar cycle variation in the

terrestrial O^+ ions is presently believed to be associated with the varying output of solar EUV radiation (Ref. 20). Because the ISEE spacecraft were launched during the rising phase of the latest solar cycle, and because the ISEE-1 ion mass spectrometer acquired data well through the peak of this cycle, the observations may have been biased towards peak occurrence of O^+ ions.

Results obtained for ions other than the O^+ are perhaps less dramatic but they contain significant new information nevertheless. The results obtained for the H^+ and He^{++} in the plasma sheet (Figures 1, 2 and 7), for instance, show that the H^+ often has nearly the same energy-per-nucleon spectrum as the He^{++} but varies in spectral shape relative to the He^{++} and can occassionally have almost the same energy-per-charge spectrum as the He^{++}. Similar energy-per-nucleon spectra would be expected if the H^+ and He^{++} were of solar wind origin and were given mass- and charge-independent velocity increments during injection, in accordance with certain "merging" models, but the latter results show that a significant portion of the plasma sheet kinetic energies may have other origins as well.

The ISEE-1 data on the O^+ and other ions are not only of great intrinsic value but they have also proved to contain crucial information for the interpretation of data from some of the other instruments on ISEE-1 and -2. It is necessary, for example, to know the ion mass distribution in order to interpret magnetic pulsations (Ref. 48) and to calculate E x B drifts from observed particle flux distributions (Refs. 57 and 58).

8. RECOMMENDATIONS

On the whole the ISEE mission has already been highly successful in integrating observations from many different kinds of experiments and this may well be the particular strength of this international undertaking. With the vast data base now available from the ISEE-1 ion mass spectrometer and all the other ISEE-1, -2, and -3 experiments it is of utmost importance that these cooperative efforts be continued over the next several years.

9. REFERENCES

1. Balsiger, H., P. Eberhardt. J. Geiss, A. Ghielmetti, H. P. Walker, D. T. Young, H. Loidl, and H. Rosenbauer, "A satellite-borne ion mass spectrometer for the energy range 0 to 16 keV", Space Sci. Instrum., 2, 499, 1976.

2. Shelley, E. G., R. D. Sharp, R. G. Johnson, J. Geiss, P. Eberhardt, H. Balsiger, G. Haerendel, and H. Rosenbauer, "Plasma composition experiment on ISEE-A", IEEE Trans. Geosci. Electr., GE-16, 266, 1978.

3. Shelley, E. G., D. A. Simpson, T. C. Sanders, E. Hertzberg, H. Balsiger, and A. Ghiemetti, "The energetic ion composition spectrometer (EICS) for the Dynamics Explorer-A", Space Sci. Inst., 5, 443, 1981.

4. Baugher, C. R., C. R. Chappell, J. L. Horwitz, E. G. Shelley, and D. T. Young, "Initial thermal plasma observations from ISEE-1", Geophys. Res. Lett., 7, 657, 1980.

5. Horwitz, J. L., C. R. Baugher, C. R. Chappell, E. G. Shelley, and D. T. Young, "Pancake pitch angle distributions in warm ions observed with ISEE-1", J. Geophys. Res., 86, 3311, 1981.

6. Schmidt, W. K. H., H. Rosenbauer, E. G. Shelley, and J. Geiss, "On temperature and speed of He^{++} and O^{6+} ions in the solar wind", Geophys. Res. Lett., 7, 697, 1980.

7. Ghielmetti, A. G., R. G. Johnson, R. D. Sharp, and E. G. Shelley, "The latitudinal diurnal, and altitudinal distributions of upward flowing energetic ions of ionospheric origin, Geophys. Res. Lett., 5, 59, 1978.

8. Gorney, D. J., A. Clarke, D. Croley, J. F. Fennell, J. Luhman, and P. F. Mizera, "The distribution of ion beams and conics below 8,000 km", J. Geophys. Res., 86, 83, 1981.

9. Collin, H. L., R. D. Sharp, E. G. Shelley, and R. G. Johnson, "Some general characteristics of upflowing ion beams over the auroral zone and their relationship to auroral electrons", J. Geophys. Res., 86, 6820, 1981.

10. Schunk, R. W. "Mathematical structure of transport equations for multispecies flows", Rev. Geophys. Space Phys. 15, 429-445, 1977.

11. Hones, E. W., Jr., J. R. Asbridge, S. J. Bame, M. D. Montgomery, S. Singer, and S. I. Akasofu, "Measurements of magnetotail plasma flow made with VELA 4B", J. Geophys. Res., 77, 5503, 1972.

12. Rosenbauer, H., H. Grunwaldt, M. D. Montgomery, G. Paschmann, and N. Schopke, "IEOS-2 plasma observations in the distant polar magnetosphere: The plasma mantle", J. Geophys. Res., 80, 2723, 1975.

13. Hardy, D. A., H. K. Hills, J. W. Freeman, Jr., "A new plasma regime in the distant geomagnetic tail", Geophys. Res. Lett., 2, 169, 1975.

14. Frank, L. A., K. L. Ackerson and D. M. Yeager, "Observations of atomic oxygen (O^+) in the earth's magnetotail", J. Geophys. Res., 82, 129, 1977.

15. Shelley, E. G., "Ion composition in the dayside cusp: Injection of magnetosheric ions into the high latitude boundary layer", Proceedings of Magnetospheric Boundary Layers Conference, Alpbach, 11-15 June, 1979 (ESA SP-148, August 1979).

16. Peterson, W. K., R. D. Sharp, E. G. Shelley, and R. G. Johnson, "Energetic ion composition of the plasma sheet", J. Geophys. Res., 86, 761, 1981.

17. Sharp, R. D., W. Lennartsson, W. K. Peterson, and E. G. Shelley, "The origins of the plasma in the distant plasma sheet", J. Geophys. Res., 87, 10420, 1982.

18. Kamei, T., and H. Maeda, "Auroral electrojet indices (AE) for January-June 1978", World Data Center for Geomagnetism, Data Book No. 3, Kyoto University, April, 1981.

19. Shelley, E. G., R. G. Johnson, and A. Ghielmetti, Relationship of upward flowing energetic ions to geomagnetic activity (abstract), EOS, 61, 1080, 1980.

20. Young, D. T., H. Balsiger, and J. Geiss, "Correlations of magnetospheric ion composition with geomagnetic and solar activity", J. Geophys. Res., 87, 9077, 1982.

21. Hundhausen, A. J., Coronal Expansion and Solar Wind, p. 99, Springer-Verlag Berlin-Heidelberg, 1972.

22. Balsiger, H., P. Eberhardt, J. Geiss, and D. T. Young, "Magnetic storm injection of 0.9-16 keV/e solar and terrestrial ions into the high altitude magnetosphere", J. Geophys. Res., 85, 1645, 1980.

23. Johnson, R. G., "A review of the hot plasma composition near geosynchronous altitude in Spacecraft Charging Technology 1980, Conference Proceedings edited by N. J. Stevens and C. P. Pike, p. 412, NASA-CP-2182, 1981.

24. Lennartsson, W., and R. D. Sharp, "Relative contribution of terrestrial and solar wind ions in the plasma sheet, Advances in Space Research, in press, 1985.

25. Akasofu, S.-I., Physics of Magnetospheric Substorms, D. Reidel, Boston, 1977.

26. Lennartsson, W., R. D. Sharp, and R. D. Zwickl, "Substorm effects on the plasma sheet ion composition on March 22, 1979 (CDAW-6)", J. Geophys. Res., 90, 1243, 1985.

27. Sharp, R. D., D. L. Carr, W. K. Peterson, and E. G. Shelley, "Ion streams in the magnetotail", J. Geophys. Res., 86, 4639, 1981.

28. Hardy, D. A., J. W. Freeman and H. K. Hills, "Plasma observations in the magnetotail", in Magnetospheric Particles and Fields, edited by B. M. McCormac, p. 89, D. Reidel, Dordrecht, Holland, 1976.

29. Hardy, D. A., H. K. Hills, and J. W. Freeman, "Occurrence of lobe plasma at lunar distance", J. Geophys. Res., 84, 72, 1979.

30. Crooker, N. V., "Dayside merging and cusp geometry", J. Geophys. Res., 84, 951, 1979.

31. Pillip, W. G., and G. Morfill, "The formation of the plasma sheet resulting from plasma mantle dynamics", J. Geophys. Res., 83, 5670, 1978.

32. Ashour-Abdalla, M., H. Okuda, and C. Z. Cheng, "Acceleration of heavy ions on auroral field lines", Geophys. Res. Lett., 8, 795, 1981.

33. Kindel, J. M., and C. F. Kennel, "Topside Current Instabilities", J. Geophys. Res., 76, 3055, 1971.

34. Johnson, R. G., R. D. Sharp, and E. G. Shelley, "Observations of ions of ionospheric origin in the storm time ring current", Geophys. Res. Lett., 4, 403, 1977.

35. Shelley, E. G., R. G. Johnson, and R. D. Sharp, "Satellite observations of energetic heavy ions during a geomagnetic storm", J. Geophys. Res., 77, 6104, 1972.

36. Lennartsson, W., R. D. Sharp, E. G. Shelley, R. G. Johnson, and H. Balsiger, "Ion composition and energy distribution during 10 magnetic storms", J. Geophys. Res., 86, 4678, 1981.

37. Lennartsson, W., E. G. Shelley, R. D. Sharp, R. G. Johnson, and H. Balsiger, "Some initial ISEE-1 results on the ring current composition and dynamics during the magnetic storm of December 11, 1977", Geophys. Res. Lett., 6, 483, 1979.

38. McIlwain, C. E., "Plasma convection in the vicinity of the geosynchronous orbit", in Earth's Magnetospheric Processes, edited by B. M. McCormac, p. 268, D. Reidel, Dordrecht, Holland, 1972.

39. Smith, P. H. and R. A. Hoffman, "Ring current particle distributions during the magnetic storms of December 16-18, 1971", J. Geophys. Res., 78, 4731, 1973.

40. Williams, D. J., "Ring current composition and sources", in Dynamics of the magnetosphere, S.-I. Akasofu, editor, Reidel, 1980.

41. Lennartsson, W. and R. D. Sharp, "A comparison of the near equatorial ion composition between quiet and disturbed conditions", J. Geophys. Res., 87, 6109, 1982.

42. Smith, P. H., N. K. Bewtra, and R. A. Hoffman, "Inference of the ring current ion composition by means of charge exchange decay", J. Geophys. Res., 86, 3470, 1981.

43. Smith, P. H., and N. K. Bewtra "Charge exchange lifetimes for ring current ions", Space Sci. Rev., 22, 301, 1978.

44. Lyons, L. R., and D. S. Evans, "The inconsistency between proton charge exchange and the observed ring current decay", J. Geophys. Res., 81, 6197, 1976.

45. Tinsley, B. A., "Evidence that the recovery phase ring current consists of helium ions", J. Geophys. Res., 81, 6193, 1976.

46. Sharp, R. D., W. Lennartsson, and R. J. Strangeway, "The ionospheric contribution to the plasma environment in near-earth space, Radio Science, 20, in press, 1985.

47. Collin, H. L., R. D. Sharp, E. G. Shelley, "The magnitude and composition of the outflow of energetic ions from the ionosphere", J. Geophys. Res., 89, 2185-2194, 1984.

48. Singer, H. J., C. T. Russell, M. G. Kivelson, T. A. Fritz, and W. Lennartsson, Geophys. Res. Lett., 6, 889, 1979.

49. Peterson, W. K., E. G. Shelley, R. D. Sharp, R. G. Johnson, J. Geiss, and H. Rosenbauer, "H^+ and He^{++} in the dawnside magnetosheath", Geophys. Res. Lett., 6, 667, 1979.

50. Peterson, W. K., E. G. Shelley, G. Haerendel and G. Paschmann, "Energetic ion composition in the subsolar magnetopause and boundary layer", J. Geophys. Res., 87, 2139, 1982.

51. Scholer, M. F., M. Ipavich. G. Gloecker, D. Hovestadt, and B. Klecker, "Leakage of magnetospheric ions into the magnetosheath along reconnected field lines at the dayside magnetopause", J. Geophys. Res., 86, 1299, 1981.

52. Speiser, T. W., D. J. Williams, and H. A. Garcia, "Magnetospherically trapped ions as a source of magnetosheath energetic ions", J. Geophys. Res., 86, 723, 1981.

53. Freeman, J. W., H. K. Hills, T. W. Hill, P. H. Reiff, and D. A. Hardy, "Heavy ion circulation in the earth's magnetosphere", Geophys. Res. Lett., 4, 195, 1977.

54. Lundin, R., L. R. Lyons, and N. Pissarenko, "Observations of ring current composition at L < 4", Geophys. Res. Lett., 7, 425, 1980.

55. Young, D. T., "Ion composition in magnetospheric modeling", in Quantitative Magnetospheric Models, R. Olsen (Editor) Am. Geophys. Union, Washington, D. C., 1979.

56. Lennartsson, W., and R. D. Sharp, "Solar cycle effects on the plasmasheet ion composition, (abstract), EOS, 65, 1051, 1984.

57. Candidi, M., S. Orsini, and A. G. Ghielmetti, "Observations of multiple ion beams in the magnetotail: evidence for a double proton population, J. Geophys. Res., 89, 2180, 1984.

58. Orsini, S., M. Candidi, V. Formisano, H. Balsiger, A. Ghielmetti, and K. W., Ogilvie, "The structure of the plasma sheet-lobe boundary in the earth's magnetotail", J. Geophys. Res., 89, 1573, 1984.

ACKNOWLEDGMENTS

We wish to acknowledge the important contributions to the Plasma Composition Experiment by a number of people. In particular the design, development, and calibration of the instrument and the subsequent analysis of the energetic ion data were all due in major parts to the combined efforts of E. G. Shelley, W. K. Peterson, R. G. Johnson, D. L. Carr and A. Ghielmetti of the Lockheed Palo Alto Research Laboratory; C. R. Chappell of the Marshall Space Flight Center; H. Balsiger, J. Geiss, and P. Eberhardt of the University of Bern; H. Rosenbauer and W. K. H. Schmidt of the Max-Planck Institut in Lindau; and G. Haerendel and G. Paschman of the Max-Planck Institut in Garching.

We also wish to thank C. T. Russell of the University of California at Los Angeles for use of the data from the ISEE-1 magnetometer.

Finally we wish to express our sincere gratitude towards the personnel of the ISEE Project Office at NASA Goddard Space Flight Center, especially R. O. Wales, for their critical technical and administrative support throughout the entire project.

BIBLIOGRAPHY

1. Papers published, in press, or submitted.

Baker, D. N., T. A. Fritz, W. Lennartsson, B. Wilken, and H. W. Kroehl, The role of heavy ionospheric ions in the localization of substorm disturbances on 22 March 1979: CDAW-6, J. Geophys. Res., 90, 1273, 1985.

Balsiger, H., Composition of hot ions (0.1-16 keV/e) as observed by the GEOS and ISEE mass spectrometers and inferences for the origin and circulation of magnetospheric plasmas, Adv. Space Res., 1, 289, 1981.

Balsiger, H., On the composition of the ring current and the plasma sheet and what it tells about the sources of these hot plasmas, in High-Latitude Space Plasma Physics, B. Hultqvist and T. Hagfors, eds., Plenum Publishing Corp. London, 313, 1983.

Candidi, M., S. Orsini, and A. G. Ghielmetti, Observations of multiple ion beams in the magnetotail: evidence for a double proton population, J. Geophys. Res., 89, 2180, 1984.

Cladis, J. B., and W. E. Francis, The polar ionosphere as a source of the stormtime ring current, J. Geophys. Res., 90, in press, 1985.

Cladis, J. B., and W. E. Francis, Transport of ions in presence of induced electric field and electrostatic turbulence: a double-spiral injection boundary, Advances in Space Research, in press, 1985.

Eastman, T. E., L. A. Frank, W. K. Peterson, and W. Lennartsson, The plasma sheet boundary layer, J. Geophys. Res., 89, 1553, 1984.

Fritz, T. A., D. N. Baker, R. L. McPherron, and W. Lennartsson, Implications of the 1100 UT March 22, 1979, CDAW-6 substorm event for the role of magnetic reconnection in the geomagnetic tail, Magnetic Reconnection in Space and Laboratory Plasmas, E. W. Hones, Jr., Editor, Geophysical Monograph 30, American Geophysical Union, Washington, D.C., 203, 1984.

Horita, R. E., E. Ungstrup, R. D. Sharp, R. R. Anderson, and R. J. Fitzenreiter, Counterstreaming hydrogen and oxygen ions observed in the magnetosphere on ISEE-1, Advances in Space Research, in press, 1984.

Johnson, R. G., Review of the hot plasma composition near geosynchronous altitude, in Proceedings of Spacecraft Charging Technology 1980 Conference, edited by N. J. Stevens and C. P. Pike, NASA CP-2182, 412, 1981.

Lennartsson, W., and R. D. Sharp, A comparison of the 0.1-17 keV/e ion composition in the near equatorial magnetosphere between quiet and disturbed conditions, J. Geophys. Res., 87, 6109, 1982.

Lennartsson, W., E. G. Shelley, R. D. Sharp, R. G. Johnson, and H. Balsiger, Some initial ISEE-1 results on the ring current composition and dynamics during the magnetic storm of December 11, 1977, Geophys. Res. Lett., 6, 483, 1979.

Lennartsson, W., R. D. Sharp, E. G. Shelley, R. G. Johnson, and H. Balsiger, Ion composition and energy distribution during 10 magnetic storms, J. Geophys. Res., 86, 4678, 1981.

Lennartsson, W., R. D. Sharp, and R. L. Zwickl, Substorm effects on the plasma sheet ion composition on March 22, 1979 (CDAW-6), J. Geophys. Res., 90, 1243, 1985.

Lennartsson, W., and R. D. Sharp, Achievements of the plasma composition experiment on ISEE-1 during the IMS, Proc. Conf. Achievements of the IMS, ESA SP-217, 283, 1984.

Lennartsson, W., and R. D. Sharp, Relative contribution of terrestrial and solar wind ions in the plasma sheet, Advances in Space Research, in press, 1985.

Orsini, S., M. Candidi, H. Balsiger, A. Ghielmetti, Ionospheric ions in the near earth geomagnetic tail plasma lobes, Geophys. Res. Lett., 9, 163, 1982.

Orsini, S., M. Candidi, V. Formisano, H. Balsiger, A. Ghielmetti, and K. W. Ogilvie, The structure of the plasma sheet-lobe boundary in the earth's magnetotail, J. Geophys. Res., 89, 1573, 1984.

Orsini, S., E. Amata, M. Candidi, H. Balsiger, M. Stokholm, C. Huang, W. Lennartsson, and P. -A. Lindqvist, Cold streams of ionospheric oxygen in the plasma sheet during the CDAW-6 event of March 22, 1979, J. Geophys. Res., 90, submitted, 1985.

Peterson, W. K., E. G. Shelley, R. D. Sharp, R. G. Johnson, J. Geiss, and H. Rosenbauer, H^{+} and He^{++} in the dawnside magnetosheath, Geophys. Res. Lett., 6, 667, 1979.

Peterson, W. K., R D. Sharp, E. G. Shelley, and R. G. Johnson, Energetic ion composition of the plasma sheet, J. Geophys. Res., 86, 761, 1981.

Peterson, W. K., E. G. Shelley, G. Haerendel, and G. Paschmann, Energetic ion composition in the subsolar magnetopause and boundary layer, J. Geophys. Res., 87, 2139, 1982.

Schmidt, W. K., H. H. Rosenbauer, E. G. Shelley, and J. Geiss, On temperature and speed of He^{++} and O^{6+} ions in the solar wind, Geophys. Res. Lett., 7, 697, 1980.

Sharp, R. D., D. L. Carr, W. K. Peterson, and E. G. Shelley, Ion streams in the magnetotail, J. Geophys. Res., 86, 4639, 1981.

Sharp, R. D., W. Lennartsson, W. K. Peterson, and E. G. Shelley, The origins of the plasma in the distant plasma sheet, J. Geophys. Res., 87, 10420, 1982.

Sharp, R. D., W. Lennartsson, W. K. Peterson, and E. Ungstrup, The mass dependence of wave particle interactions as observed with the ISEE-1 energetic ion mass spectrometer, Geophys. Res. Lett., 10, 651, 1983.

Sharp, R. D., R. G. Johnson, W. Lennartsson, W. K. Peterson and E. G. Shelley, Hot plasma composition results from the ISEE-1 spacecraft, in Energetic Ion Composition in the Earth's Magnetosphere, edited by R. G. Johnson, Terra Scientific Publishing Co., Tokyo, Japan, and D. Reidel Publishing Co., Dordrecht, Holland, 231, 1983.

Sharp, R. D., W. Lennartsson, and R. J. Strangeway, The ionospheric contribution to the plasma environment in near-earth space, Radio Science 20, in press 1985.

Shelley, E. G., R. D. Sharp, R. G. Johnson, J. Geiss, P. Eberhardt, H. Balsiger, G. Haerendel, and H. Rosenbauer, Plasma composition experiment on ISEE-A, IEEE Trans. Geosci. Electr., GE-16, 266, 1978.

Shelley, E. G., D. A. Simpson, T. C. Sanders, E. Hertzberg, H. Balsiger and A. Ghielmetti, The energetic ion composition spectrometer (EIC) for the Dynamics Explorer-A, Space Science Instrumentation, 5, 443, 1981.

Shelley, E. G., Circulation of energetic ions of terrestrial origin in the magnetosphere, Advances in Space Research, in press, 1985.

Singer, H. J., C. T. Russell, M. G. Kivelson, T. A. Fritz, and O. W. Lennartsson, The spatial extent and structure of PC-3, -4, -5 pulsations near the magnetospheric equator, Geophys. Res. Lett., 6, 889, 1979.

Ungstrup, E., R. D. Sharp, C. A. Cattell, R. R. Anderson, R. D. Fitzenreiter, D. S. Evans, and D. N. Baker, Observation of a westward travelling surge from satellites at low, medium and high altitudes, J. Geophys. Res., 90, submitted, 1985.

2. Papers presented at meetings or seminars.

Balsiger, H., P. Eberhardt, J. Geiss, D. T. Young, R. G. Johnson, W. Lennartsson, R. D. Sharp, and E. G. Shelley, The composition of the hot magnetospheric plasma during the 11 December 1977 geomagnetic storm as observed by three satellites, EOS, 60, 928, 1979.

Cladis, J. B., and W. E. Francis, Transport of stochastically accelerated H^+ and O^+ ions in the magnetosphere during magnetic storms, EOS, 63, 1075, 1982.

Cladis, J. B., and W. E. Francis, Effects of energy diffusion and charge-transfer loss on distributions of H^+ and O^+ ions convected inward from the plasma sheet, EOS, 64, 299, 1983.

Cladis, J. B., and W. E. Francis, Transport of ions from the auroral ionosphere to the inner magnetosphere during stormtime conditions, IAGA Bulletin No. 48, 327, 1983.

Cladis, J. B., and W. E. Francis, Evidence that the polar ionosphere is the principal source of the stormtime ring current, EOS, 64, 806, 1983.

Cladis, J. B., and W. E. Francis, Transport of ions in presence of induced electric field and electrostatic turbulence: a double-spiral injection boundary, presented at the XXVth COSPAR Meeting in Graz, Austria, 25 June - 7 July, 1984.

Eastman, T. E., L. A. Frank, W. K. Peterson, and E. G. Shelley, The plasma sheet boundary layer, EOS, 61, 1071, 1980.

Ghielmetti, A., H. Balsiger, J. Geiss, D. T. Young, E. G. Shelley, R. G. Johnson, R. D. Sharp, W. K. Peterson, and H. Rosenbauer, Characteristics of ion streams in the magnetotail from ISEE-1, EOS, 60, 929, 1979.

Ghielmetti, A., H. Balsiger, D. T. Young and P. Eberhardt, Composition of ion populations in the earth's magnetotail, EOS, 61, 1080, 1980.

Huang, C. Y., L. A. Frank, W. K. Peterson, G. K. Parks, W. Lennartsson and R. J. Decoster, Filamentary plasma distributions in the geomagnetic tail lobes, EOS, 64, 812, 1983.

Huang, C. Y., L. A. Frank, W. K. Peterson, D. J. Williams, W. Lennartsson, D. G. Mitchell, R. C. Elphic, and C. T. Russell, Filamentary structures in the magnetotail. To be presented at the Chapman Conference on Magnetospheric Polar Cap, Fairbanks, Alaska, August 6-9, 1984.

Johnson, R. G., W. Lennartsson, R. D. Sharp, E. G. Shelley, and H. Balsiger, The composition of the near equatorial ring current during the December 11, 1977, magnetic storm, EOS, 59, 1163, 1978.

Johnson, R. G., W. Lennartsson, E. G. Shelley, R. D. Sharp, and H. Balsiger, Signatures of ring current injection processes in the ion energy spectra from the ISEE-1 plasma composition experiment, EOS, 60, 348, 1979.

Johnson, R. G., W. Lennartsson, R. D. Sharp, E. G. Shelley, H. Balsiger, P. Eberhardt, J. Geiss, and D. T. Young, Multiple satellite observations of the hot plasma composition during the 21-22 February 1979 geomagnetic storms, EOS, 60, 928, 1979.

Lennartsson, W., Recent results from the ISEE-1 plasma composition experiment, Seminar given at the Royal Institute of Technology, Stockholm, December, 1979.

Lennartsson, W., ISEE-1 measurements of the magnetospheric ion composition at $R \leq 15\ R_E$, VII. MPAE Lindau Workshop on Ionic Composition, August 26-29, 1980.

Lennartsson, W., R. G. Johnson, R. D. Sharp, E. G. Shelley, and H. Balsiger, A comparison of the storm time ion composition at different local times as measured by the ISEE-1 mass spectrometer, EOS, 61, 343, 1980.

Lennartsson, W., and E. G. Shelley, Spectral characteristics of energetic terrestrial ions as measured by the ISEE-1 mass spectrometer, EOS, 61, 1080, 1980.

Lennartsson, W., R. D. Sharp, and E. G. Shelley, Mass and energy distribution of ions with energies below 17 keV/e at the inner edge of the ring current, EOS, 62, 995, 1981.

Lennartsson, W., and R. D. Sharp, A comparison between ion composition data and predictions based on charge exchange decay, EOS, 63, 403, 1982.

Lennartsson, W., and R. D. Sharp, Substorm effects on the plasma sheet ion composition on March 22, 1979, IAGA Bulletin No. 48, A3, 1983.

Lennartsson, W., and R. D. Sharp, Substorm effects on the plasma sheet ion composition, Seminar given at the Royal Institute of Technology, Stockholm, August, 1983.

Lennartsson, W., and R. D. Sharp, Composition and energy distribution of 0.1-16 keV/e ions in the plasmapause region, presented at the conference on Fundamental Magnetospheric Processes in the Plasmapause Region, Huntsville, Alabama, October 25-27 (invited), 1983.

Lennartsson, W., and R. D. Sharp, Plasma sheet ion composition and energy distribution between 10 and 23 R_E, EOS, 64, 806, 1983.

Lennartsson, W., and R. D. Sharp, Recent results on magnetospheric ion composition, Seminar given at the University of Maryland, College Park, April 30, 1984.

Lennartsson, W., and R. D. Sharp, Achievements of the plasma composition experiment on ISEE-1 during the IMS, presented at the XXVth COSPAR Meeting in Graz, Austria, 25 June - 7 July, 1984.

Lennartsson, W., and R. D. Sharp, Relative contribution of terrestrial and solar wind ions in the plasma sheet, presented at the XXVth COSPAR Meeting in Graz, Austria, 25 June - 7 July, 1984.

Lennartsson, W., and R. D. Sharp, Solar cycle effects on the plasma sheet ion composition, EOS, 65, 1051, 1984.

Orsini, S., M. Candidi, V. Formisano, F. Mozer, K. Ogilvie, and A. Ghielmetti, Structure of the plasma lobe-plasma sheet interface in the geomagnetic tail at 22 R_E, IAGA Bulletin No. 45, 394, 1981.

Orsini, S., E. Amata, M. Candidi, H. Balsiger, M. Stokholm, C. Huang, W. Lennartsson, P. A. Lindqvist, and G. Paschmann, Cold ionospheric O^+ beams in the inner plasma sheet during the March 22, 1979 substorms, IACA Bulletin No. 48, A3, 1983.

Orsini, S., K. vonBurg, and H. Balsiger, The plasma sheet properties as observed by the ISEE-1 ion composition experiment, EOS, 65, 263, 1984.

Paschmann, G., D. H. Fairfield, E. W. Hones, Jr., C. Huang, W. Lennartsson, and S. Orsini, Plasma signatures of substorm activity in the magnetotail: ISEE-1 and -2 observations on March 22, 1979, IAGA Bulletin No. 48, A2 (invited), 1983.

Peterson, W. K., E. G. Shelley, R. D. Sharp, R. G. Johnson, J. Geiss, and H. Rosenbauer, Composition of ion streams in the subsonic magnetosheath observed on ISEE-1, EOS, 59, 1164, 1978.

Peterson, W. K., R. D. Sharp, E. G. Shelley, R. G. Johnson, and H. Balsiger, On the origin of the plasma sheet, EOS, 60, 345, 1979.

Peterson, W. K., E. W. Hones, Jr., E. G. Shelley, R. D. Sharp, H. Balsiger, S. Bame, and G. Paschmann, Measurements of O^+ and He^{++} in the low latitude boundary layer from ISEE-1, EOS, 60, 929, 1979.

Peterson, W. K., R. D. Sharp, E. G. Shelley, R. G. Johnson, A. Ghielmetti, and H. Rosenbauer, Observations of accelerated ionospheric ions in the magnetotail lobes from ISEE-1, AGU Chapman Conference on the Formation of Auroral Arcs, Fairbanks, Alaska, July 21-25, 1980.

Peterson, W. K., R. D. Sharp, E. G. Shelley, R. G. Johnson, and H. Balsiger, Energetic ion composition of the plasma sheet, EOS, 61, 343, 1980.

Peterson, W. K., E. G. Shelley, E. W. Hones, Jr., S. J. Bame, and G. Paschmann, Mass composition of the magnetospheric boundary layer, EOS, 61, 1079, 1980.

Peterson, W. K., E. G. Shelley, G. Paschmann, and G. Haerendel, On the origin of the subsolar magnetospheric boundary layer, IAGA Bulletin No. 45, 416, 1981.

Peterson, W. K., E. G. Shelley, G. Haerendel, and G. Paschmann, Energetic ion composition in the subsolar magnetopause and boundary layer, EOS, 62, 995, 1981.

Peterson, W. K., E. G. Shelley, W. K. H. Schmidt, P. Bochsler, and H. Balsiger, Correlated measurements of minor ions in the solar wind and dayside cusp, IAGA Bulletin No. 48, 416, 1983.

Schmidt, W. K. H., H. Rosenbauer, E. G. Shelley, and P. Eberhardt, On the properties of O^{6+} ions in the solar wind, EOS, 60, 363, 1979.

Schmidt, W. K. H., H. Rosenbauer, E. G. Shelley, and J. Geiss, On the properties of He^{2+} and O^{6+} ions in the solar wind, EOS, 60, 931, 1979.

Schmidt, W. K. H., H. Rosenbauer, J. Geiss, and E. G. Shelley, On superheating and velocity differences of heavy ions in the solar wind, EOS, 62, 1018, 1981.

Schmidt, W. K. H., ISEE-1 results on heavy minor ions in the solar wind, IAGA Bulletin No. 48, 411, 1983.

Sharp, R. D., E. G. Shelley, R. G. Johnson, W. K. Peterson, A. Ghielmetti, and H. Rosenbauer, Composition of ion streams in the magnetotail, EOS, 60, 348, 1979.

Sharp, R. D., W. Lennartsson, R. G. Johnson, E. G. Shelley, and H. Balsiger, An overview of ISEE-1 mass spectrometer data on the ring current ion population (E/Q $\lesssim$ 17 keV/e) during magnetic storms, EOS, 60, 929, 1979.

Sharp, R. D., and W. Lennartsson, A comparison of the ion composition in the near equatorial magnetosphere during quiet and disturbed conditions, EOS, 61, 1080, 1980.

Sharp, R. D., R. G. Johnson, W. Lennartsson, W. K. Peterson, and E. G. Shelley, Hot plasma composition results from the ISEE-1 spacecraft, 4th IAGA Scientific Assembly, Edinburgh, August 3-15 (invited), 1981.

Sharp, R. D., W. Lennartsson, E. G. Shelley, and W. K. Peterson, ISEE measurements of plasma sheet ion composition, EOS, 62, 995, 1981.

Sharp, R. D., W. Lennartsson, W. K. Peterson, and E. G. Shelley, Substorm associated effects on the average energies of plasma sheet ions of different species, EOS, 63, 1075, 1982.

Sharp, R. D., Ion composition in the magnetotail, EOS, 64, 291 (invited), 1983.

Sharp, R. D., W. Lennartsson, W. K. Peterson, and E. Ungstrup, Evidence for an epithermal tail in the phase space density distribution of ions tranversely accelerated in the high altitude auroral ionosphere, EOS, 64, 801, 1983.

Sharp, R. D., and E. G. Shelley, Terrestrial ion source for the dynamic plasma sheet, EOS, 65, 1051, 1984.

Shelley, E. G., W. K. Peterson, G. Haerendel, G. Paschmann, and H. Balsiger, On the origin of the magnetospheric boundary layer plasma, EOS, 59, 1163, 1978.

Shelley, E. G., W. K. Peterson, R. D. Sharp, R. G. Johnson, J. Geiss, and H. Rosenbauer, H^{+} and He^{++} in the dawnside magnetosheath, EOS, 60, 348, 1979.

Shelley, E. G., Circulation of energetic ions of terrestrial origin in the magnetosphere, presented at the XXVth COSPAR Meeting in Graz, Austria, 25 June - 7 July, 1984.

Singer, P. J., W. J. Hughes, C. T. Russell, W. Lennartsson, N. C. Maynard, and F. S. Mozer, The harmonic of resonant hydromagnetic waves, EOS, 62, 358, 1981.

Ungstrup, E., R. D. Sharp, C. A. Cattell, R. R. Anderson, R. J. Fitzenreiter, D. S. Evans, and D. N. Baker, Particle and wave observations at a discontinuity in the magnetosphere associated with a westward travelling surge, IAGA Bulletin No. 48, 374, 1983.